Evolution and Development of the Stickleback Lateral Line

Margaret Grace Mills

A dissertation

submitted in partial fulfillment of the

requirements for the degree of

Doctor of Philosophy

University of Washington

2013

Reading Committee:

Catherine L. Peichel, Chair

David W. Raible

Cecilia B. Moens

Program Authorized to Offer Degree:

Molecular and Cellular Biology

University of Washington

Abstract

Evolution and Development of the Stickleback Lateral Line

Margaret Grace Mills

Chair of the Supervisory Committee:
Professor Catherine L. Peichel
Department of Biology

The lateral line sensory system allows fish to sense water movement. It has been implicated in many behaviors, including schooling, prey detection and capture, and rheotaxis. The number and arrangement of neuromasts in the lateral line varies substantially between populations of the threespine stickleback (*Gasterosteus aculeatus*). In some cases, variation in the lateral line is correlated with variation in ecological habitat, suggesting that it may be adaptive. Previous work in the Peichel lab identified differences between the adult lateral line patterns of two stickleback populations, a marine population from Japan (JP) and a freshwater benthic lake population from British Columbia (PB), as well as the genetic architecture of those differences. The most striking differences between these two populations are in the number and patterning of

neuromasts in the main posterior (Mp) trunk line. For my thesis research, I investigated the developmental and genetic basis of the differences in Mp. PB fish have more neuromasts than JP in the Mp line, and this difference maps to Chromosome XXI. In Chapters 2 and 3, I used a number of techniques to try to identify the gene within the region responsible for the difference in number: recombination mapping, analysis of individual candidate genes, RNA-seq analysis of all genes in the region, and *in situ* hybridization. I did not identify the causative gene, but I did show that the candidate gene *Eya1* is expressed in neuromasts during stickleback development. I also demonstrated that difference in neuromast number between PB and another freshwater population does not map to Chromosome XXI, suggesting that there are other loci that control neuromast number in sticklebacks. A second difference in the Mp line, the arrangement of neuromasts, correlates strongly with the presence of bony lateral plates and maps to Chromosome IV. In Chapter 4, I found that the elaboration of the neuromast pattern coincides with the growth of those plates through postembryonic development. I also used transgenesis to demonstrate that pleiotropic activity of the gene responsible for plate development, *Eda*, is also responsible for the difference in neuromast pattern.

Table of Contents

List of Figures

List of Tables

Acknowledgements

Thank you to the other members of the Peichel Lab who contributed to this research:

Abby Wark, who started mapping lateral line phenotypes in the PBxJP F2 cross, and who taught me how to DASPEI stain

Anna Greenwood, who was heavily involved in making and injecting the Eda constructs and phenotyping the transgene-injected fish, who answered all of my questions with patience and great intelligence, and who gives the best pep talks in the history of pep talks

Mike White, who wrote most of the scripts used to analyze the RNA-seq data, and who provided patient answers to my many bioinformatics and statistics questions

Matt Dubin, Lam-Ha Dang, Rebecca Bruders and Amy Sullivan, for helping to genotype and phenotype HTxPB F2 fish

Shaun McCann, for fish care

Jen Cech and James Urton, Matt Arnegard, and honorary lab members Mia Levine and Nitin Phadnis for helpful comments in lab meetings.

Thank you to Katie Peichel for welcoming me into her lab with open arms, for supporting me through two pregnancies and numerous bumps in the research road, and for making her lab such a positive place to work.

Thank you to my committee members for many excellent suggestions over the years, and in particular to my reading committee for helping me improve this thesis.

Thank you to the MCB program, both the directors (Dave Raible and Michael Emermann) and the administrative staff (Michele Karantsavelos, MaryEllin Robinson, Terry Duffy, and Diane Darling) for help with numerous issues through the years, and for being friendly faces and cheerful advocates.

Thank you to Pam Lindberg, Elizabeth Jensen, Luna Yu, Pat Heath, and the many other people at the Fred Hutchinson Cancer Research Center who make research at the Hutch so much easier.

Thank you to my parents, Paul and Claire Grace, for being enthusiastic and supportive through every step of grad school and through my entire education.

Thank you to my husband, James Mills, without whom I might not have joined the Peichel lab, and without whom I certainly wouldn't have finished grad school.

Dedication

To Hayden and Rowan,
Who constantly remind me to investigate the world with joy, wonder, and determination.
I love you.

Chapter 1 – Introduction

Dear frog and fish, or newt and shark,
You needn't worry when it's dark;
You'll escape or dine just fine
Svenning with your lateral line.

Poem in honor of Sven Dijkgraaf, who first described the function of the lateral line [1]

A breathtaking amount of work, both descriptive and experimental, has been put into the analysis of embryonic development. Although we know much about the genes involved in embryonic development, much of the genetic basis of postembryonic development remains a mystery [2, 3]. Furthermore, the phenotypic differences that set related species apart are often manifest only in postembryonic stages (the second half of the so-called morphological "hourglass" [4]), and so even less is known about the genetic and developmental mechanisms responsible for phenotypic evolution. It is the development and evolution of adult phenotypes that is of particular interest to me. Broadly, I have asked several questions in my research: How do similar-looking babies grow up into different-looking adults? What are the developmental changes that result in phenotypic differences between species? What genes underlie these phenotypic differences, and when and how do they act?

I approached these questions using the lateral line system as a model. This is the organ system that mediates the *Ferntastsinn*, or sense of touch at a distance for many fish and

aquatic amphibians, allowing them to sense movement in the water around their bodies [5-7]. The lateral line has been implicated in a wide range of postembryonic behaviors, particularly for fishes. These include interactions with the abiotic environment, such as identifying and navigating around stationary objects [5, 8, 9] and maintaining position in flowing water (rheotaxis) [10-13]. They also include interactions with the biotic environment, in detecting and localizing prey [14-18], detecting and avoiding predators [19], attracting and competing for mates [20, 21], and most classically, schooling [22-24].

The sensing components of the lateral line are clusters of cells called neuromasts, which are arrayed in distinct lines on the body and head. These neuromasts are made up of several types of cells: hair cells, in the center of the neuromast, each project several stereocilia and a single kinocilium up into a gelatinous cupula that protrudes into the surrounding fluid; non-sensing support and mantle cells surround the hair cells, produce the cupula, and serve to replace damaged hair cells [25]. The bending of the cupula and the cilia in response to changes in local water pressure cause the nerves that innervate the lateral line to fire [26]. There are two general types of neuromast, and they differ in their sensitivity to movement in the water. Canal neuromasts are enclosed (as the name implies) within subsurface canals that are connected to the exterior by occasional pores; their cupulae project into the fluid that fills the canals and are therefore exposed only to water motion within the canals. By contrast, surface neuromasts are located on the exterior surface of the animal, and their cupulae project directly into the surrounding

water. These different types of neuromast therefore differ in sensitivities: canals filter out some motion, and are therefore considered to be more useful in high-flow environments than surface neuromasts, but there is some disagreement about exactly the roles of one type of neuromast relative to the other [27].

The lateral line has been a useful model system in which to study many aspects of embryonic development, including issues of cellular lineage, directed cell migration, interaction of cell types, differentiation, and the contribution of specific genes and molecules to all of these processes, particularly in the zebrafish *Danio rerio* (for reviews see [28-31]). The neuromasts of the lateral lines, and the nerves that innervate them, originate from a series of placodes [32-34]. The process is best described for the lateral line of the body, referred to as the trunk or posterior lateral line (as opposed to that of the head, the cephalic or anterior lateral line), and I will focus on this line. The anterior part of the placode forms the lateral line ganglion, and the posterior part of the placode forms the posterior lateral line primordium, which delaminates and migrates from behind the ear down the flank to the tail, dropping off protoneuromasts at regular intervals, with a string of interneuromast cells in between [30, 35, 36]. The primordioum also tows the lateral line ganglion behind it as it migrates [37], and the axons from this ganglion innervate the neuromasts as they are deposited [38]. All neuromasts deposited by the initial primordium (primI) have the same anterior-posterior axis of sensitivity, while neuromasts deposited by a second primordium (primII) all have a dorso-ventral axis of

sensitivity [39, 40], but within each neuromast two sets of hair cells are oriented in opposing directions along that axis [41, 42]. Separate afferent neurons selectively innervate hair cells with each orientation, both within and between neuromasts [43, 44]. The afferent neurons project to all rhombomeres of the embryonic hindbrain [45].

The molecular basis of postembryonic development of the posterior lateral line is much less-well explained than that of embryonic development, but cell migration and differentiation of the postembryonic lateral line has been described for zebrafish as well as a few other fishes [46-48]. The details differ between species, but a number of features are the same: additional primordia (such as primII in zebrafish) migrate along the trunk from the region of the original placode; neuromasts migrate away from the paths of the primordia; new neuromasts form by budding off existing neuromasts and/or by differentiating *de novo* from interneuromast cells left behind by the migrating primordia [40, 46, 48, 49]. For example, in postembryonic zebrafish, a second primordium (primII) deposit neuromasts in between those from primI, the neuromasts deposited by both primI and primII migrate ventrally from their sites of deposition, and any body segments left unoccupied by initial primI or primII neuromasts are then filled by interneuromast cells that differentiate into intercalary neuromasts in the same line as the migrated primI and primII neuromasts [40]. Similar deposition and migration patterns occur along the dorsal aspect of the flank, as the dorsal component of primII, primD, contributes both neuromasts and interneuromast cells [40, 46]. After these neuromasts have migrated

ventrally, additional interneuromast cells then differentiate along the lines of original deposition for both primI/primII and primD, with regulation from the lateral line-associated glia [50, 51]. Finally, these neuromasts bud off additional neuromasts into vertical patterns called stitches [46, 49, 52]. In bluefin tuna (*Thunnus thynnus*), simple changes in these processes result in a markedly different adult lateral line pattern: neuromasts are deposited by prim1 and prim2 in a manner similar to that of zebrafish, but in tuna the anteriormost neuromasts in particular migrate dorsally instead of ventrally; interneuromast cells differentiate into neuromasts in the same line as the initial (migrated) prim1 and prim2 neuromasts but not along the line of original deposition; and no budding of additional stitch neuromasts occurs [48].

The embryonic lateral lines described so far can be grouped into a very small number of categories, suggesting that embryonic lateral line patterns are conserved across species [53]. This is in dramatic contrast to the many adult lateral line phenotypes described, which show incredible diversity [54, 55]. There are differences in the number and structure of canals [55], the presence of canal vs. surface neuromasts [5, 56, 57], the number of neuromasts, either overall or in particular lines [57-60], and the size and shape of the neuromasts that are present [56, 59, 61]. There are also numerous examples in which variation in different aspects of the lateral line is associated with variation in ecological habitat [56-60, 62], suggesting that variation in the lateral line may be adaptive.

Much analysis of the evolution of lateral line patterns that has occurred between adult forms has involved describing phenotypes and mapping them onto phylogenies of the species [54, 55, 63]. These studies have led to hypotheses that lateral line morphology is limited by developmental constraints, and that heterochrony, or a change in the relative timing of different developmental steps, has been the key to effecting change within those constraints [63]. Others, using comparative developmental analyses of divergent species, have focused on the ways in which simple changes to particular aspects of development, such as the direction of migration of neuromasts away from the midline in zebrafish vs. bluefin tuna, might yield different patterns in the adults [48].

To fully test these hypotheses about the evolution of the lateral line, we need a system in which we can follow development to see when and how differences in pattern arise, identify genetic changes underlying the differences, manipulate the gene(s) to alter the phenotype and demonstrate causality, and—critically—test the effects of the differences on behavior and fitness [64-66]. Zebrafish are a very powerful system in which to examine the developmental processes and underlying genes, and they have been used for some behavioral analyses involving the lateral line [13]. However, zebrafish currently have two significant drawbacks as a system in which to study lateral line evolution. First, no naturally occurring variation in the lateral line has been identified in *D. rerio*. Second, little is known about their natural history, including the flow regimes, predators, prey, or

behaviors that might influence the evolution of their sensory capacities, or that might inform the fitness effects of any changes in lateral line pattern [67].

Lateral line patterns have been shown to vary within a few other species, all of which exhibit substantial variation in ecosystem or niche between populations. First, surface- and cave-adapted morphs of the Mexican tetra (*Astyanax mexicanus*) were shown to differ radically in the number of cranial neuromasts [68], as well as in the size and shape of those neuromasts [61]. Trinidadian guppies (*Poecilia reticulata*) show variation in the number of superficial neuromasts, particularly dorsal neuromasts, that correlates with variation in intensity of predation pressure as well as more broadly between watersheds [60]. Ninespine sticklebacks (*Pungitius pungitius*) from different populations in northern Europe have varying numbers of neuromasts, particularly anterior canal neuromasts [62]. Finally, and of greatest interest to me, threespine sticklebacks (*Gasterosteus aculeatus*) living in marine and freshwater environments show variation in both number and arrangement of neuromasts (**Figure 1-1** and [58, 69]).

Threespine sticklebacks are a particularly good system in which to study the evolution of lateral line morphology. Sticklebacks are small fish that were historically found in marine environments (estuaries and oceans) but within the last 12,000 years have invaded and adapted to freshwater environments (streams and lakes) in myriad independent watersheds throughout the northern hemisphere. These fish have a rich history as the

subjects of ecological and behavioral research, and they are well-established as a system in which to study adaptation and selection [70, 71].

The phenotypic variation observed between these recently-diverged populations is substantial, and in some cases equals or surpasses the divergence seen at the genus level in other fishes [72-74], yet they can be crossed in the laboratory to generate fertile offspring. There are many molecular, genetic and genomic tools available for use with threespine sticklebacks, including microsatellite markers and SNP (single nucleotide polymorphism) arrays, a well-annotated reference genome, and the ability to manipulate gene expression or analyze gene regulation through transgenic animals [75-79]. Using these tools (and others), crosses between phenotypically divergent populations have been used to study the genetic bases of a range of phenotypic differences [69, 73, 75, 78-84].

Before I joined the Peichel lab, Abby Wark began a project to use these tools to investigate the genetics of lateral line evolution. Threespine sticklebacks have a simple lateral line, with neuromasts arranged in twelve distinct lines of superficial neuromasts on the body and head [58, 85]. Within this simple framework, however, Abby found that adults from different populations of sticklebacks exhibit greater variation in numbers and arrangements of neuromasts than intraspecific variation that had been identified at that time aside from the surface and cave populations of *Astyanax mexicanus* [58]. She also found that some of this variation was correlated with the habitat in which the populations

lived, suggesting that the differences might be adaptive. The most striking differences between the populations surveyed were found in the Main trunk line, which in sticklebacks is divided into two lines: neuromasts found on segments of the trunk anterior to the second dorsal spine belong to the "Ma" (Main trunk, anterior) line, while those on segments of the trunk posterior to the second dorsal spine are in the "Mp" (Main trunk, posterior) line. Abby noted that the most striking difference in neuromast arrangement in these two lines correlated with the presence or absence of bony lateral plates, a trait that varies consistently and predictably in marine *vs*. freshwater environments [74, 86, 87]. Marine (completely plated) populations like the fish from the Pacific Ocean near Akkeshi, Japan (JP) have 30-36 bony plates covering their entire flanks on each side. These fish have a pair of neuromasts on each plate in this region, one located above the midline of the flank and one below the midline (**Figure 1-1a**). Most freshwater populations like the fish from Humptulips Pond, Washington (HT) are considered low-plated, and they have 6-8 bony plates on each side of their flanks, with all (or sometimes all but one) of these plates located in the region of the Ma line. In the (unplated) Mp line they generally have one or two neuromasts per body segment located on the midline (**Figure 1-1b**). Fish from the "benthic" population of sticklebacks from Paxton Lake, British Columbia, Canada (PB) have very few plates in the Ma region in addition to a lack of plates in the Mp region. These fish have a dense string of neuromasts located along the midline in both Ma and Mp, although there are a few neuromasts dorsal to the midline in the Ma line even in the absence of plates. These fish also exhibit a

proliferation of trunk neuromasts, with up to five neuromasts per body segment (**Figure 1-1c**), nearly three times as many neuromasts as JP fish have in Mp [58].

To investigate the genetic basis of these differences, Abby chose these two most divergent populations, the marine JP and the freshwater benthic PB, to use in a mapping cross. She bred a single PB female to a single JP male, then intercrossed their F1 progeny to each other to generate an F2 mapping population. She then analyzed the phenotype and genotype of each F2 fish, and identified correlation between variation in their lateral line phenotypes and particular genomic regions using QTL mapping. She demonstrated that the differences in lateral line patterns she had observed were heritable, and moreover that the genetic basis of variation in the different lines is modular [69]. She was able identify seven different genomic regions that correlated with differences in neuromast number, each of which affected a different subset of the lines. Given the differences in genic requirements observed between the cranial and trunk lateral lines in zebrafish [30], it was somewhat expected that differences in those lines would map to different chromosomes, but the genetic distinction between the number of neuromasts in Ma and Mp lines was quite surprising.

For my dissertation research, I chose to pursue the genetic and developmental mechanisms that underlie two of the most significant quantitative trait loci (QTL) Abby identified. First, I investigated the difference in neuromast number in the Mp line, which

mapped to Chromosome (Chr) XXI. I continued mapping efforts started by Abby, attempting to narrow the region of the QTL both in the original cross and in a second cross (described in Chapter 2). I then investigated the genes within that QTL, trying to identify the gene(s) responsible for causing the difference in neuromast number, using several different molecular techniques as well as next generation sequencing (described in Chapter 3). Finally, I described the development of the neuromast arrangement in the Mp line and its correlation with the development of the bony plates found in the same region. Abby had mapped the phenotypic differences in neuromast arrangement to Chr IV, where the bony plate phenotype had previously been mapped, and I used transgenic gene expression to demonstrate that one of the genes in the QTL, *Eda*, was responsible for the neuromast pattern phenotype in addition to causing the plate phenotype (described in Chapter 4).

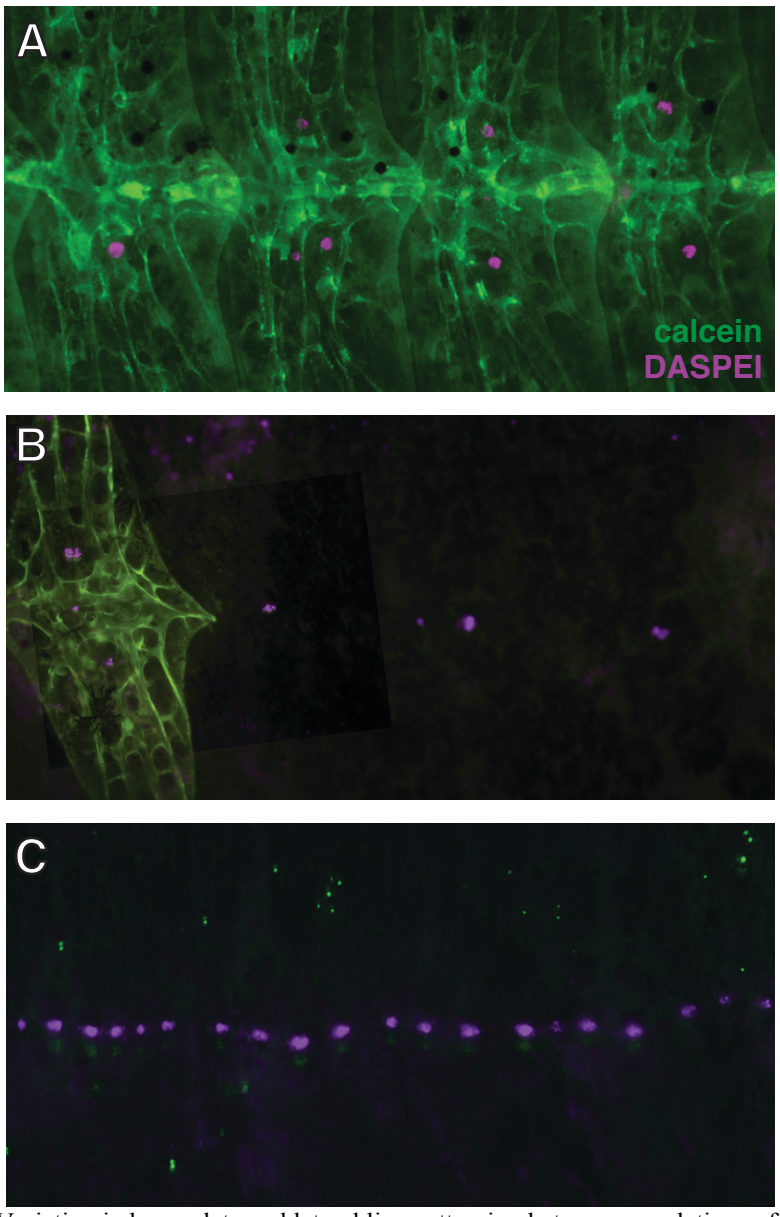

Figure 1-1. Variation in bony plate and lateral line patterning between populations of threespine stickleback.
(A-C) Four body segments from an individual of each population, costained to visualize bony plates (green, stained with calcein) and neuromasts (purple, stained with DASPEI). In all pictures, dorsal is up and rostral is to the left.
(A) Pacific Ocean, Akkeshi, Japan "JP"; (B) Humptulips Pond, Washington State, USA "HT"; (C) benthic population from Paxton Lake, British Columbia, Canada "PB".

Chapter 2 – Genetic analysis of variation in neuromast numbers between threespine stickleback populations

Parts of this chapter were published in [69]

1. Introduction

Neuromasts are the sensory units of the lateral line, and changes in the number of neuromasts may affect the way in which a fish perceives motion in its environment. Neuromast numbers have been shown to vary between closely related species of fish [57, 59], and even between different populations of the same species [58, 60, 62, 68]. In some cases, variation in neuromast number within or between species is correlated with variation in ecological factors. For example, neuromast number is correlated with exposure to waves in species of triplefin fishes (*Forsterygion* and *Notoclinops* spp.) [59], and with predation intensity in populations of Trinidadian guppies (*Poecilia reticulata*) [60]. Thus, variation in neuromast number may have evolved as an adaptation to different ecological conditions.

Previous work in the Peichel lab revealed that threespine sticklebacks vary in number of neuromasts depending on the population of origin. In particular, benthic populations of fish from two freshwater lakes in British Columbia, Canada, (Paxton and Priest lakes, PB and RB) have more neuromasts than fish from the limnetic populations from the same

lakes, and indeed they have more neuromasts than fish from any other populations surveyed [58]. The results of a QTL mapping study, correlating genotype with lateral line phenotypes in F2 individuals from the cross of a PB female with a Japanese marine (JP) male, revealed interesting modularity to this difference: variation in the number of neuromasts from different lines mapped to different places in the genome [69]. Surprisingly, different genetic loci underlie the number of neuromasts on trunk segments anterior to the second dorsal spine (the "Ma" line) vs. those on trunk segments posterior to the second dorsal spine (the "Mp" line). The difference in neuromast number in the Mp line was the largest observed between JP (**Figure 1-1a**) and PB fish (**Figure 1-1c**), and one of the largest observed between any populations surveyed: PB fish have nearly three times as many neuromasts in Mp as do JP fish [58, 69]. The difference in neuromast number in the Mp line maps to a QTL on Chr XXI that has a large phenotypic effect, explaining 36% of the variance in the phenotype [69]. Because the difference in phenotype was so dramatic, my goal was to identify the gene(s) responsible for differences in Mp neuromast number within the Chr XXI QTL. The large number of neuromasts in each unplated Mp segment of PB (and RB) fish is unusual in threespine sticklebacks [58], which led to the hypothesis that neuromast number in the Mp line was a constructive trait: selectively increased in the PB population, rather than a regressive trait that was selectively reduced in the JP population.

Several strategies were used to try to identify the gene(s) underlying the observed difference in neuromast number. First, more genetic markers and more individuals were added to the analysis in an attempt to narrow the QTL region. Second, the same chromosomal region was investigated in a second cross in the hopes that it would avoid some of the pitfalls encountered in working with the first mapping cross. These approaches were not successful in substantially refining the Chr XXI QTL, so molecular analysis of genes in this region was used to determine whether any were responsible for the difference in neuromast number between JP and PB fish (see Chapter 3).

2. Results and Discussion

A. Genetic mapping in the PBxJP F2 cross

Originally, 234 PBxJP F2 fish were genotyped using single nucleotide polymorphism (SNP) arrays [76], which contained several markers within the region of the QTL on Chr XXI. We first attempted to refine the QTL by genotyping at additional microsatellite markers in this region of Chr XXI (**Table 6-1**). Unfortunately, not enough fish were recombinant in the region of interest for additional markers to provide much additional resolution: out of 234 fish used in the original study, only 157 of these had phenotype data for Mp; of these, only 2 fish out of the original 234 had recombination events between markers at 5.7 Mb and 7.9 Mb, while 8 had recombination between markers at 4.5 Mb and 5.7 Mb (the majority of the region of the QTL). Therefore, phenotypic

variation mapped to a broad stretch of Chr XXI: markers across the first 9.5 Mb out of 11.7 Mb of Chr XXI all had LOD scores above the genome-wide significance threshold of 3.7 for Mp neuromasts [69] and markers from 4.0 Mb to 7.9 Mb had LOD scores within 1.5 LOD of the peak at 7.9 Mb (**Figure 2-1a**).

Since adding additional markers did not help resolve the QTL interval, more individuals were added to the data set. A potentially confounding locus was present nearby: a QTL for plate number in the region of the Mp line, previously identified as a modifier of the primary plate-number-controlling locus on Chr IV [80], mapped to Chr XXI with a peak at 4.5 Mb [69]. Since the presence of plates has a slight effect on neuromast number [69], it is possible that the gene(s) controlling neuromast number on Chr XXI could be affected by this plate modifier locus, as well as being linked to it. Because of the possibility that there was a second locus in the region affecting the phenotype we were studying, and because the highest calculated LOD score for neuromast number occurred at the 7.9 Mb marker, which is distal to the QTL for plate number at 4.5 Mb, an attempt was made to separate the neuromast number QTL from the plate modifier QTL by adding more fish that were recombinant between 4.5 Mb and 7.9 Mb. Therefore, an additional 40 fish were added to the mapping population, enriched for individuals that were recombinant between those markers (see Methods). Of these fish, 6 had recombination events between 5.7 Mb and 7.9 Mb, and 1 had a recombination event between 4.5 Mb and 5.7 Mb. The

remaining fish either had recombination events outside of this region, or were nonrecombinant throughout the region of Chr XXI that was genotyped.

Rather than genetically separate the plate modifier locus from a neuromast number locus as was hoped, these extra recombinant fish appeared to shift the QTL for neuromast number away from the marker at 7.9 Mb and toward the marker at 4.0 Mb (**Figure 2-1a)**. The low number of recombinants between 4.5 Mb and 5.7 Mb in the added fish may have contributed to this shift. Additional recombinants between these two markers may help resolve the two suspected peaks or may provide more confidence in the width of the QTL for neuromast number.

The additional fish had a lower average number of neuromasts in Mp than the fish from the original mapping cross (original fish: 38.2 ± 1.3 (n=157); new fish: 23.1 ± 2.1 (n=40); Mann-Whitney U Test; $U_A = 1159.5$; $p<0.0001$), which may have inhibited the effectiveness of the new fish in narrowing the QTL. Variable DASPEI staining may have contributed to the lower neuromast numbers observed in these new fish. The quality of DASPEI staining is variable in sticklebacks, owing to differences in background staining and vital dye uptake by the neuromasts, or to susceptibility of the neuromasts to changes in water quality in their static aquaria ([69], MM and A. Greenwood, pers. observation; c.f. zebrafish housed in flow-through tank systems with consistent water quality, K. Owens, pers. communication). These individuals were phenotyped before the extent to

which this staining variability could affect the number of observable neuromasts was fully appreciated. Within the new fish alone, total neuromast number in Mp did not map to this region of Chr XXI, although average number of neuromasts per segment, a measure that is more robust to missing data because it ignores segments in which no neuromasts were observed, did cross the conservative genome-wide LOD significance threshold of 4.2 [69] from the markers at 1.9 Mb to 7.0 Mb (**Figure 2-1b**).

B. Genetic mapping in the HTxPB F2 cross

Within the QTL region on Chr XXI, the PB and JP fish have a large chromosomal inversion with respect to each other (breakpoints at 5779893-5789748 Mb and 7482685-7486832 Mb [77]), which partially explains why we could not further resolve the QTL interval by recombination mapping in the PBxJP F2 cross. To get around the difficulty in genetic mapping caused by this inversion, a second mapping cross was made between a PB male and a female from the Humptulips Pond, Washington (HT) population. HT fish have several advantages over JP as a population to cross with PB to look for a locus that controls neuromast number. First, HT fish have the same inversion state on Chr XXI as PB fish [77], so the chance of detecting recombination events within the region was higher. Second, HT is a low-plated population with at most one plate occurring in Mp, so neither the epistatic plate number locus on Chr IV nor its modifier locus on Chr XXI can obscure the effects of the neuromast number locus on Chr XXI. Finally HT fish have 1-2

neuromasts per segment in Mp (**Figure 1-1b**), so their phenotype is quite different from that of PB fish.

As expected, fish from this cross exhibited a relatively higher rate of recombination across the QTL interval on Chr XXI than fish from the PBxJP cross: the markers at 5.7 and 7.9 Mb are separated by only 0.5 cM in the PBxJP cross but by 2.9 cM in the HTxPB cross (**Figure 2-2a**). Unfortunately for this study, the variation in neuromast number between HT and PB populations showed no correlation with genotype on Chr XXI, as measured at microsatellite markers in the region (**Table 5-1**). This is not due to a lack of phenotypic variation in the HTxPB cross: F2 fish from the HTxPB cross exhibit a total phenotypic range comparable to that of the original PBxJP F2 fish (**Figure 2-2b**). However, the average number of neuromasts in HTxPB F2s was higher than in the PBxJP cross (PBxJP fish: 38.2 ± 1.3 (n=157); HTxPB fish: 58.3 ± 1.4 (n=129); Mann-Whitney U Test; $U_A = 16907$; $p<0.0001$), and the distribution was unimodal whereas it was bimodal in the PBxJP cross. It is probably also not due to the direction of the cross (the PB fish was the male grandparent in the HTxPB cross, instead of the female grandparent as in the PBxJP cross), as preliminary mapping of neuromast number in 73 fish from a PBxHT F2 cross also showed no linkage to markers at 5.7 Mb or 7.9 Mb on Chr XXI (data not shown). A genome-wide QTL analysis to identify loci that underlie the variation in neuromast number between these two populations is ongoing.

The large number of neuromasts in each unplated segment of PB fish is unusual in threespine sticklebacks, appearing only in the two benthic lake populations out of the 16 populations previously surveyed [58]. This suggests that the locus on Chr XXI should be a "constructive" trait, an alteration specific to the PB population that increases neuromast number over that in other populations, rather than a "regressive" trait that reduces the number of neuromasts in the JP population [69]. This hypothesis is challenged by the finding that variation in neuromast number does not map to Chr XXI in the HTxPB cross: a constructive genetic change to increase the number of Mp neuromasts in PB relative to the numbers in other populations would be expected to also appear as underlying the difference in neuromast number between PB and HT populations, but this was not the case. It is possible that the presence of plates in Mp in the PBxJP cross, influenced by the plate modifier locus on Chr XXI, has a greater effect on Mp neuromast number in this cross than was initially apparent: the interaction of genotypes between Chr IV (the primary gene driving plate number, *Eda*) and Chr XXI on neuromast number in Mp was not significant [69], but the effect of total plate number as determined by genotype at *Eda* and at the modifier loci on Chr VII and Chr XX, and especially at the modifier locus on Chr XXI [80], may affect the number of Mp neuromasts that form. The near absence of plates in the region of the Mp line in both HT and PB fish means the plate-forming loci cannot influence neuromast number; therefore, the gene(s) underlying the difference in neuromast number between HT and PB populations may reveal additional mechanisms for neuromast development and/or proliferation in threespine sticklebacks. Mapping the

trait in this cross may also answer the question of whether the higher number of Mp neuromasts in PB is a constructive or regressive trait: once an underlying locus is identified in the HTxPB cross, that region can be compared to JP and other populations to determine which is the ancestral and which is the derived form. Comparison of the Chr XXI region in the other benthic lake population (RB) might aid in identifying the causal difference between PB and JP or between PB and HT, if the same difference is responsible for increased neuromast number in RB and PB. Analysis of neuromast number in additional stickleback populations might also help to determine whether the elevated number of Mp neuromasts in PB and RB is as unique as it appeared from Abby's original population survey [58].

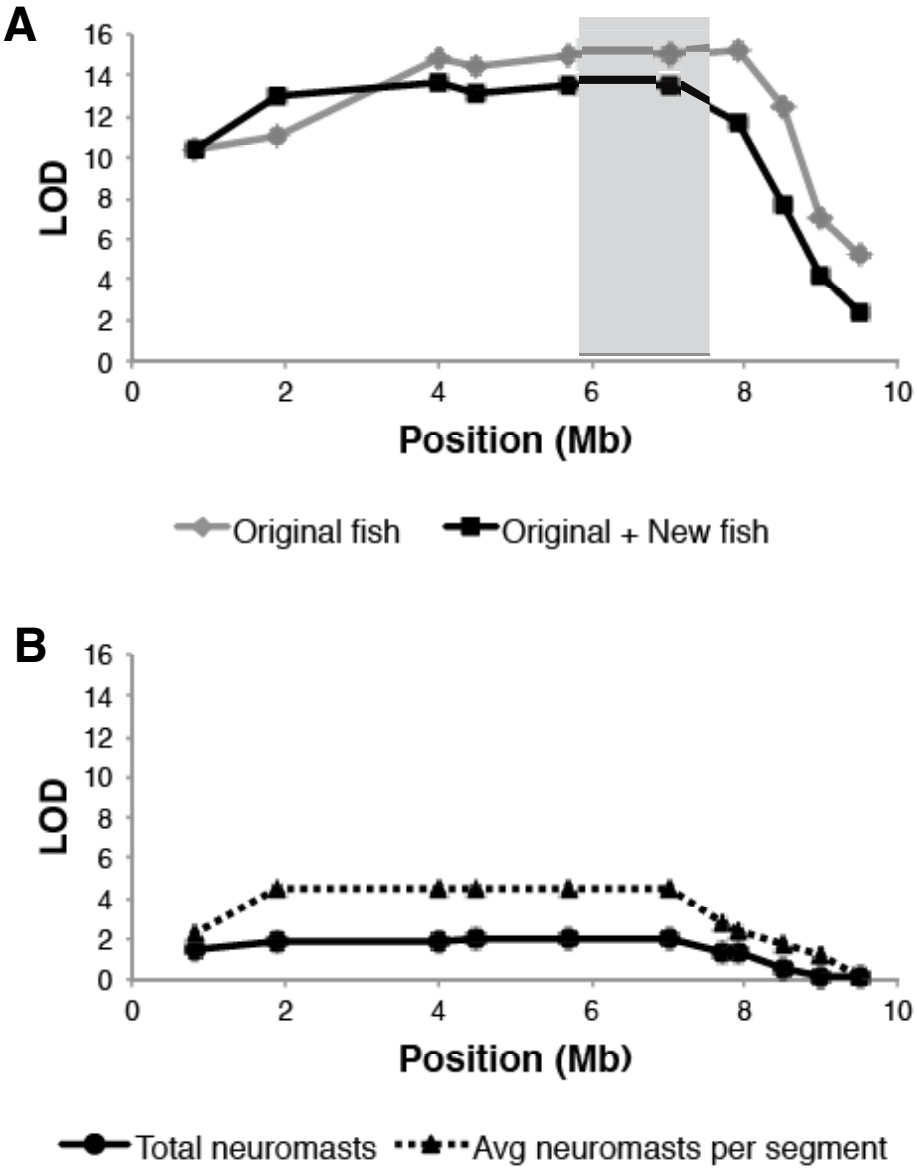

Figure 2-1. Mapping neuromast number to Chr XXI in the PBxJP F2 cross.
(A) Linkage map of the QTL for neuromast number: LOD score at each genetic marker for original fish and for original fish plus new individuals. Light grey panel shows the location of the genomic inversion on Chr XXI between PB and JP (5.8-7.5 Mb).
(B) Linkage map for new PBxJP individuals: LOD score at each genetic marker for total number of neuromasts in Mp and for average number of neuromasts per body segment in Mp (calculated by dividing the number of neuromasts by the number of body segments in which neuromasts were observed).

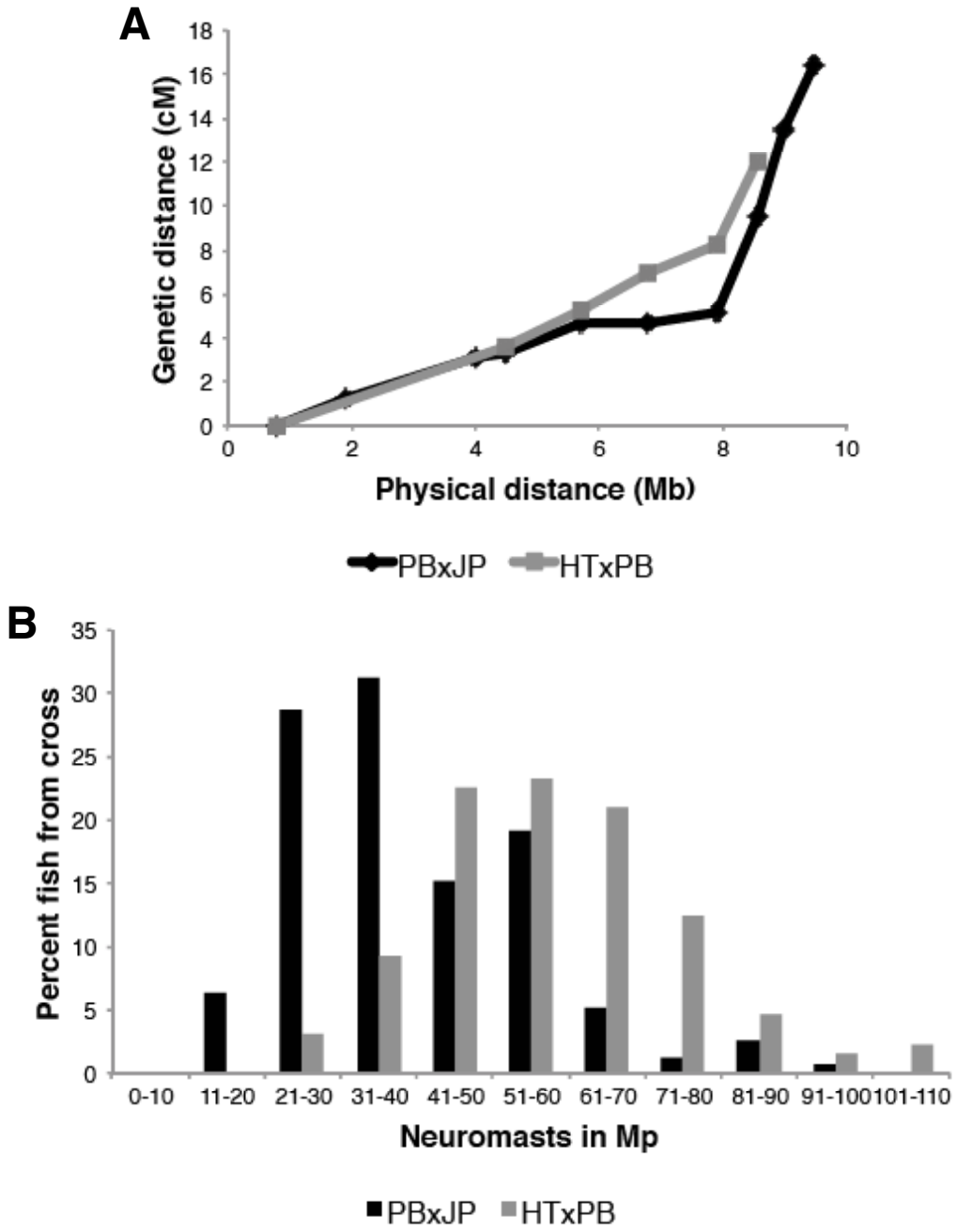

Figure 2-2. Comparison of variation in neuromast number in the HTxPB F2 cross to the PBxJP F2 cross.
(A) HT and PB have the same inversion state in Chr XXI, unlike PB and JP fish, so there is more recombination observed in the HTxPB cross in the region of the inversion (5.8-7.5 Mb).
(B) HTxPB F2s have a total phenotypic range of neuromast numbers similar to PBxJP F2s, but with a higher average and unimodal instead of bimodal distribution.

Chapter 3 – Analysis of candidate genes for variation in neuromast number between threespine stickleback populations

1. Introduction

In parallel with efforts to narrow the genetic region on Chr XXI responsible for the difference in neuromast number in the Mp line between PB and JP populations (Chapter 2), a candidate gene approach was employed. Most of the phenotypic differences between stickleback populations that have been described so far have been correlated with differences in gene expression, rather than with differences in coding sequence [77-79, 88], so this investigation focused on the relative expression levels of the genes within the QTL for neuromast number. RNA was sampled at both 2 weeks post-hatch (wph, ~12 mm standard length), when the neuromast phenotypes for the two populations are identical, and at 4wph (~17 mm standard length), when the differences between the phenotypes of the two populations have started to appear. The goal was to find a gene that was: (1) differentially expressed between the two populations at one or both ages; (2) expressed in F1 hybrids in a manner consistent with the regulatory change acting in *cis* rather than in *trans*; and (3) expressed in a spatial pattern that might indicate its contribution to the difference in neuromast number.

2. Results and Discussion

A. RNA-seq analysis

Next generation sequencing of cDNA (RNA-seq) from the PB and JP 2wph and 4wph trunk samples, with two biological replicates of each group, was used to compare expression levels of all Ensembl-predicted genes between 3.0 Mb and 7.9 Mb on Chr XXI, regardless of predicted function. Because there was no *a priori* expectation of when the responsible gene might be acting to increase neuromast numbers in PB (or to limit the increase of neuromasts in JP), genes that were differentially expressed at either 2wph or 4wph, or both, were selected for further analysis. Out of 157 predicted genes in the interval, 17 were expressed differently (adjusted $p<0.01$) between the two populations at 4wph, and two of these were also differentially expressed at 2wph (**Table 3-1**, e.g. **Figure 3-1a**), based on edgeR [89] comparisons of the number of sequencing reads from each population mapped to the gene using the program TopHat [90] (see Chapter 6). Ten of those were more highly expressed in JP fish, and seven were more highly expressed in PB fish. The number of reads from each allele at every fixed SNP within the gene was then compared in F1 RNA-seq pools. Equal expression of the two parental alleles in the F1 would suggest that the difference in gene expression between the parental populations results from differences in *trans*-acting factors elsewhere in the genome, while differential expression of the two parental alleles in the F1 suggests that changes in the *cis*-regulatory elements of that gene are responsible. Eight of the original 17 genes had

allele-specific expression patterns in the F1 that matched this latter description, indicating that *cis*-regulatory changes are likely responsible for differential expression of that gene in the parental populations. Four of these genes were expressed at least twofold as strongly in one population as in the other and also showed similarly biased allele-specific expression in F1 RNA, indicating *cis*-regulatory differences between the populations. These four genes (*MSRB2*, *CMBL*, and the novel genes ENSGACG00000002373 and ENSGACG00000002443) were therefore promising candidates for the linkage of neuromast number to the QTL on Chr XXI (e.g. **Figure 3-1b**), and were selected for confirmation.

B. Analysis of candidate genes by qPCR and pyrosequencing

In addition to the four genes selected based on RNA-seq analysis above, seven genes from the QTL interval, including the lateral line associated gene *Eya1*, were selected based on their predicted function. A twelfth gene, *SHARPIN*, had expression levels that were less dramatically different between JP and PB samples in the RNA-seq analysis, but it was also an intriguing candidate based on its predicted function as a cofactor of *Eya1*, and it was therefore included in the analysis. Relative quantities of mRNA from each of these 12 genes were compared between JP and PB populations using quantitative PCR (qPCR) (**Table 3-2**, e.g. **Figure 3-1c**). For three of the genes selected based on RNA-seq, the data generated by qPCR confirmed the conclusion from RNA-seq analysis that they were differentially expressed: MSRB2 (2wph: $p = 0.0026$; 4wph: $p < 0.0001$); CMBL

(2wph: $p < 0.0001$; 4wph: $p < 0.0001$); and the novel gene ENSGACG00000002373 (2wph: $p < 0.0001$; 4wph: $p < 0.0001$). (No qPCR primers could be found for ENSGACG00000002443, so it was only tested by pyrosequencing.) Of the eight genes (including *SHARPIN*) tested by qPCR because of their function, only two (*SOCS6* and *CPA6*) were found to be differentially expressed at both 2wph and 4wph, and this apparent difference in expression was found to be caused by SNPs in the primer sequences in the JP allele of each gene.

Relative expression of JP and PB alleles in F1 RNA was measured using pyrosequencing of a single SNP for each gene [91]. For three of the original genes, this allowed confirmation of the RNA-seq results that JP alleles for each gene were more highly expressed in F1 RNA than PB alleles (**Table 3-2**, e.g. **Figure 3-1d**): MSRB2 (2wph: $p < 0.0001$; 4wph: $p < 0.0001$); CMBL (2wph: $p < 0.0001$; 4wph: $p < 0.0001$); and the novel gene ENSGACG00000002373 (2wph: $p < 0.0001$; 4wph: $p < 0.0001$). JP and PB alleles for the fourth gene, ENSGACG00000002443, were equally expressed in F1 RNA as measured by pyrosequencing.

Thus, these analyses yielded three genes that were confirmed as being differentially expressed between JP and PB populations, and for which there was evidence of *cis*-regulatory changes in expression: *MSRB2*, *CMBL*, and the novel gene ENSGACG00000002373.

C. Analysis of candidate genes by *in situ* hybridization

The spatial expression patterns of these three candidate genes was next examined using *in situ* hybridization, in the hopes of finding some that were expressed in the region of the lateral line and might therefore be able to affect neuromast proliferation in the Mp line. Two additional genes were examined as well. The first, *Eya1*, was not shown to be differentially expressed by qPCR or pyrosequencing, but was nevertheless a gene from the QTL on Chr XXI that had been shown to play a role in neuromast development in zebrafish [92]. The second, *TROY*, located on Chr 1, is a possible receptor for the ligand *EDA* [93] (which is responsible for the development of lateral plates [94] and lateral line pattern (see Chapter 4)). Previous work in the lab had demonstrated that *TROY* is expressed in the lateral line; therefore the *TROY* probe was included as a positive control.

The *Eya1* probe stained all neuromasts (**Figure 3-2a-d**), as expected based on its expression in zebrafish [95]. Its expression patterns matched those that had been observed using DASPEI staining of live fish (**Figure 4-1e-k** and data not shown): from hatch to 2wph, lateral lines from both PB and JP fish look identical, with a single neuromast per body segment in Mp, and (by 2wph) a single neuromast above the original neuromast per segment in the anterior of Ma (**Figure 3-2a, c**). By 4wph the difference between JP and PB in neuromast phenotypes in Ma and Mp lines is apparent. In JP fish, additional neuromasts have been added dorsal and ventral to the original neuromast in

body segments at both the anterior and posterior ends of the Mp line, where plate formation is occurring (**Figure 3-2b**) (see Chapter 4). In PB fish, additional neuromasts have been added along the midline in between the original neuromasts in each body segment (**Figure 3-2d**).

TROY was expressed strongly in the neuromasts as well as the interneuromast cells, both in Mp and in all other lines (**Figure 3-2e-h** and data not shown). It appeared in a line connecting each neuromast to the next along the midline in 2wph fish from both the JP and PB populations, with additional staining of neuromasts that were located above and below the midline (**Figure 3-2e, g**). In 4wph JP fish, however, staining of the neuromasts above and below the midline remained while staining of the midline or any neuromasts on it had disappeared from the region around the Ma/Mp boundary, where plate formation was progressing (**Figure 3-2f**). Together, these probes give beautifully clear pictures of the developmental state of the lateral line at the time points surveyed, illustrating the developmental processes leading to the adult differences in neuromast number and pattern between the populations that had been previously observed ([69] and Chapters 2 and 4).

The probe for the novel gene ENSGACG00000002373 resulted in what appeared to be some staining near the midline (near the surface and cellular in appearance) in 4wph JP fish (**Figure 3-3a-d**) compared to fainter background staining that did not appear to be at

the surface or cellular in appearance, in the same region in the sense control (**Figure 3-3e-f**). There was no evidence of staining at 2wph in either population, or at 4wph in PB fish (**Figure 3-3g-h**).

Probes for *MSRB2* and *CMBL* failed to yield any staining, despite repeated attempts using varying conditions. Sense probes, used as negative controls for each antisense probe, all showed no staining, as did a no-probe control.

Neuromasts are small structures compared to the size of a fish's body, so the patterns of differential expression observed in qPCR and pyrosequencing results from trunk RNA might reflect differences in organs other than the lateral line. Therefore, when probes for *MSRB2* and *CMBL* failed to yield any staining on the skin of either JP or PB fish, RNA was collected from skin and the qPCR assay was repeated in the hopes that the differences in expression detailed above could be confirmed in samples where the neuromasts made up a larger proportion of the tissue. All five genes tested (*MSRB2*, *CMBL*, and the novel gene ENSGACG00000002373, as well as *Eya1* and *SHARPIN*) were more highly expressed in trunk RNA than in skin RNA (**Table 3-3**, **Figure 3-1e**). This was particularly striking for *MSRB2*, which was expressed 200-fold more highly in trunk RNA than skin RNA (**Table 3-3**). This was somewhat surprising given that no specific staining was observed beneath the skin for any of the probes, but could be

because the *in situ* hybridization conditions (particularly the proteinase K digestion) were optimized for detection of RNAs in the skin of the fish.

Despite this lower expression in skin, the relative expression of all five genes between the two populations were compared at both 2wph and 4wph in the skin by qPCR. Both *MSRB2* and the novel gene ENSGACG00000002373 were more highly expressed in JP than PB skin at 4wph, as they had been in whole trunk. Surprisingly, *CMBL* was more highly expressed in PB skin than JP skin at both 2wph and 4wph, unlike its relative expression in whole trunk (**Figure 3-1f**).

Three genes that were identified by the initial analysis of differential expression by RNA-seq (*MSRB2*, *CMBL*, and the novel gene ENSGACG00000002373) showed signs of being good candidates throughout the analyses performed: they were differentially expressed in parental population RNA, and their alleles were differentially expressed in F1 RNA. Embryonic expression patterns of the zebrafish homologs of all three genes were examined in a high-throughput screen of *in situ* probes, and for all three the expression is described as "not spatially restricted" [96], but none of these probes were used at postembryonic stages, and none of these expression patterns have been altered in zebrafish (by mutants or morpholinos) to see what structures would be affected. *Methionine sulfoxide reductase B2* (*MSRB2*) is an enzyme involved in protecting tissue from oxidative damage. It is expressed in human skin, including in the epidermis,

melanocytes, and sebaceous glands, and it is highly expressed in the retina and retinal pigmented epithelium in the mammalian eye [97]. Its dramatically lower expression in the skin than in the rest of the trunk (**Table 3-3**) suggests that its primary activity is somewhere other than in the lateral line and surrounding tissues.

Carboxymethylbutinolidase (*CMBL*) is a hydrolase enzyme that is expressed broadly in human tissues, and was shown to be responsible for the activation of the blood pressure-reducing prodrug olmesartan medoxomil in the human liver and intestine [98]. Digestive capacity and liver processing ability could certainly differ between marine and freshwater populations of sticklebacks, and it is relatively easy to imagine how *CMBL* might play a role in this difference through its higher level of expression in JP trunk below the skin, which could have driven the differences in expression observed in both RNA-seq and qPCR on RNA from trunk. However, the reversal in relative expression in the skin compared to the trunk (**Figure 3-1f**) suggests that *CMBL* may have different effects in the skin of PB fish, although further work is necessary to determine what those effects are.

Finally, the sequence of the novel gene ENSGACG00000002373 (as obtained from assembled RNA-seq reads) is most closely related to the predicted sequence of *transmembrane protein 56* (*TMEM56*) from a number of fish species (including *Oryzias latipes*, *Takifugu rubripes*, and *Danio rerio*), which lacks any published annotations of its function. The staining observed in 4wph JP fish with the antisense probe to this gene needs to be confirmed, but if it is real, its location in regions near the developing plates of JP fish suggests that this may be a candidate for the plate modifier locus mentioned

(Chapter 2) and reported previously [69, 80]. Such a modifier of plate development might also influence neuromast number [69].

The genes that underlie variation in number of neuromasts have not been well-studied in any system. However, there are a few genes within the Chr XXI QTL that have been shown to play a role in neuromast development in other systems and thus were considered as candidates for the increase in neuromast numbers seen in PB fish. Zebrafish with reduced *eya1* expression show decreased numbers of neuromasts, primarily attributed to increased cell death in the migrating lateral line primordia, as well as other phenotypes [92]. It is possible that an increase in *Eya1* expression in the PB primordium itself, while too small (or too early) to be picked up in the qPCR assays used here because of the tiny size of the primordium and neuromasts in relation to the size of the whole trunk, may nevertheless increase the number of interneuromast cells deposited by the primordium that are competent to develop into neuromasts. The difference in Mp neuromast number between JP and PB fish does not appear until shortly after 2wph, when additional neuromasts appear in each body segment in PB (on the midline around the original neuromast) and continue to increase in number beyond the two dorso-ventral neuromasts per segment that appear in JP. This suggests that the difference in neuromast number is due to variation in the differentiation of interneuromast cells rather than in the deposition of neuromasts [50, 51]. The greater number of Mp neuromasts in PB could be either be due to the deposition of more interneuromast cells in PB or to the differentiation

of more of those interneuromast cells into neuromasts in PB, and it is possible that *Eya1* is involved in either the deposition or differentiation processes.

A second intriguing candidate gene in the QTL, *SHANK-associated RH domain interactor* (*SHARPIN*), is expressed in osteoclasts and osteoblasts in mice and humans [99], and may interact with *Eya1* [100]. The gene was not differentially expressed between JP and PB populations in RNA isolated from either whole trunk (**Tables 3-1** and **3-2**) or skin (**Table 3-3**), but its expression level did not differ between trunk and skin (**Table 3-3**), suggesting that it is at least transcribed in the appropriate region to be involved in the difference in neuromast number. Unfortunately, efforts to clone *SHARPIN* for use as an *in situ* hybridization probe were unsuccessful, but it remains a promising candidate for future work.

The analyses reported here were focused on identifying a gene with *cis*-regulatory differences in expression between JP and PB populations, with an expression pattern that could explain the difference in neuromast number observed between the two populations. There are still reasons to explore the roles that the candidate genes discussed above may play in this difference. There are also several explanations for why these analyses did not identify the gene that underlies the neuromast number difference. First, only one program (edgeR) was used to identify differentially expressed genes, and perhaps a different algorithm would identify the gene(s) missed in this analysis. Indeed, a preliminary

analysis of the same RNA-seq data with the program cuffDiff [101] returned a similar but non-identical list of differentially expressed genes (data not shown). Second, as discussed above, neuromasts are very small structures relative to the size of the developing stickleback body, and therefore differences in gene expression that result in substantial differences in the number of neuromasts may nevertheless be disguised by equivalent levels of expression of the same gene in other tissues. Third, while there are good reasons to suspect that the difference in neuromast number is related to a difference in expression of a gene or genes, it is possible that the causative difference is coding instead of regulatory. Sticklebacks exhibit a high level of genetic diversity between populations [76], and many SNPs were identified between JP and PB in the genes examined here (**Table 3-1**), some of which result in changes to the amino acid sequence of the encoded proteins. However, sequence analysis of the coding regions for three genes (*Eya1*, *SOCS6*, and *CPA6*) indicated that the coding sequence changes for each of these genes between JP and PB were uncorrelated with neuromast phenotypes in those populations: for example, the coding sequence for *SOCS6* differs in seven amino acids out of 536 between PB and JP, but is identical between PB and HT at all seven of those positions despite the difference in neuromast number between PB and HT (data not shown). High-throughput analysis methods would be helpful in examining the RNA-seq reads to identify coding differences between the PB and JP for the rest of of the genes within the QTL for neuromast number, although as demonstrated by the *SOCS6* example,

identification of coding changes between PB and JP alone does not prove the coding change is a good candidate to cause the difference in neuromast number.

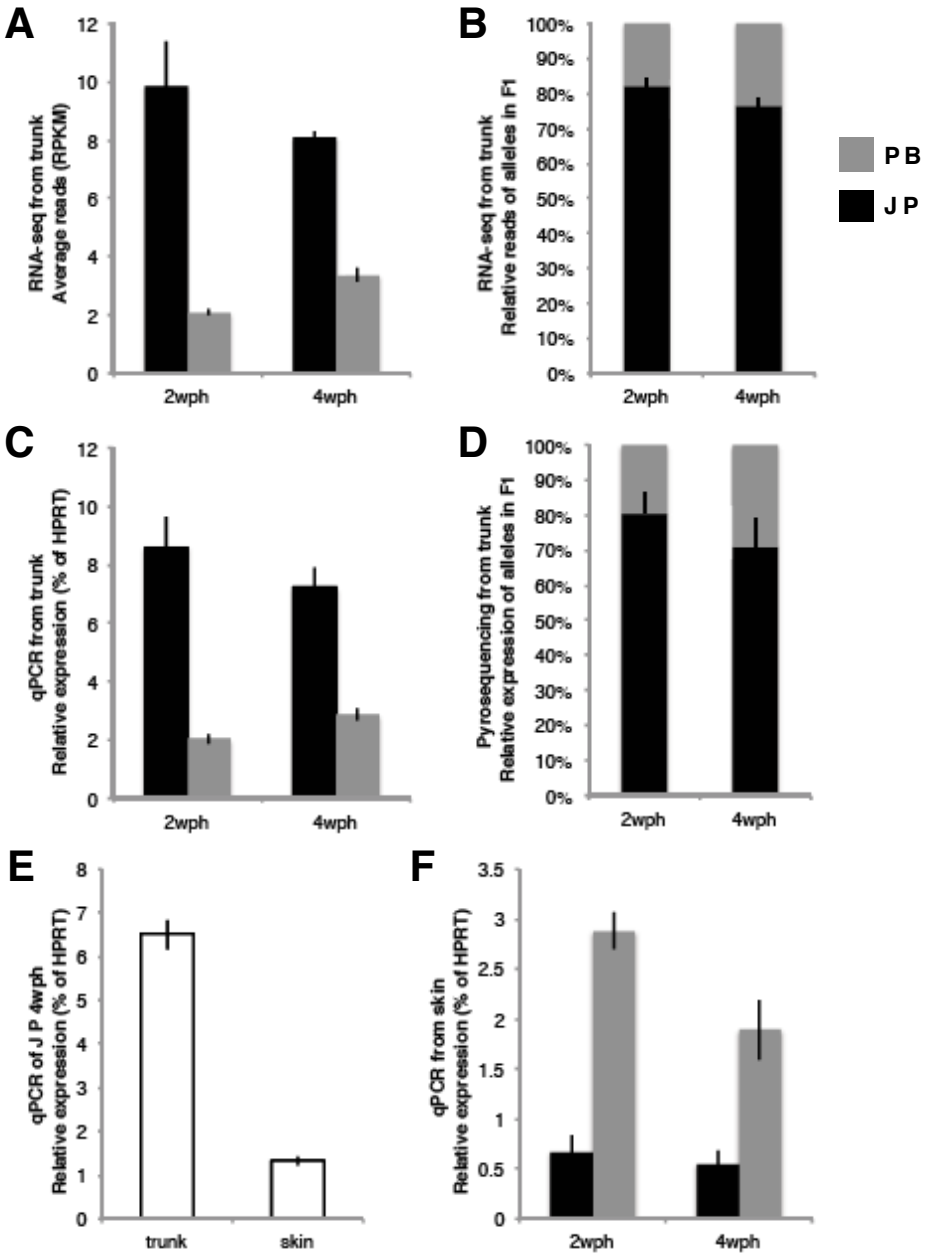

Figure 3-1. Expression of the candidate gene CMBL as measured by various analyses.
(A) Normalized reads (RPKM) from PB and JP RNA-seq pools, averaged across the two pools from each population and age. (B) Relative expression of PB and JP alleles in the two RNA-seq F1 pools from each age, averaged across all 5 fixed SNPs from the transcripts. (C) Expression level in trunk RNA, as measured by qPCR, compared to the reference gene HPRT. (D) Relative expression of PB and JP alleles in F1 trunk RNA, as measured by pyrosequencing. (E) Relative expression of CMBL in trunk vs. skin RNA from JP fish at 4wph. (F) Expression level in skin RNA, as measured by qPCR, compared to the reference gene HPRT.

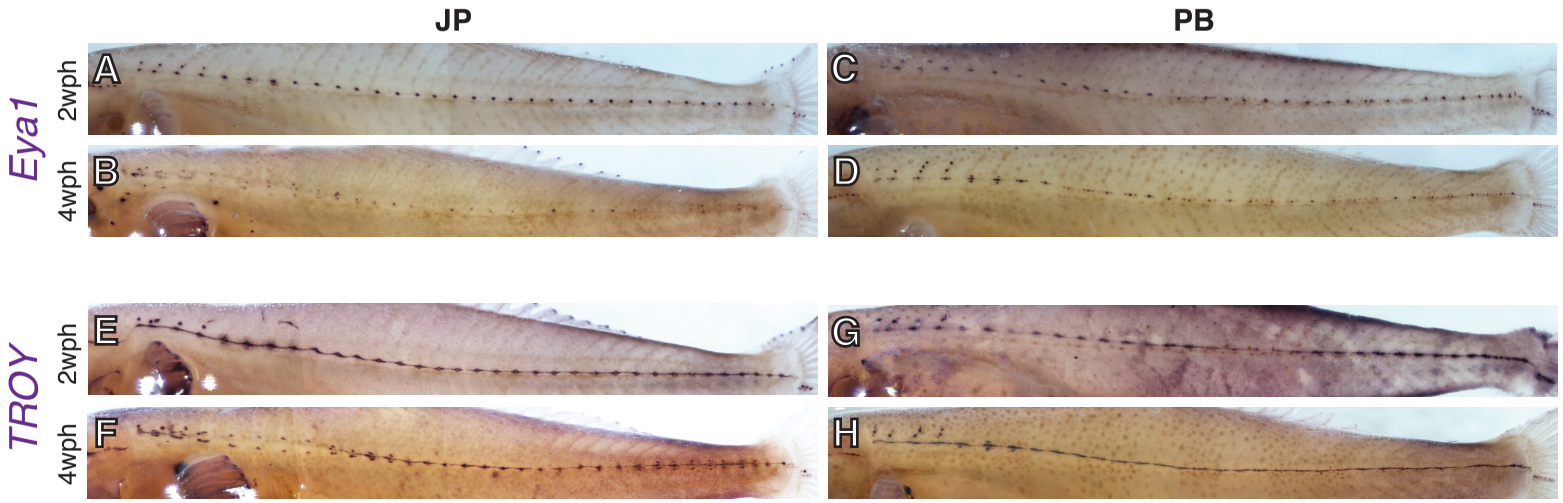

Figure 3-2. TROY and Eya1 are expressed in the lateral line of both JP and PB fish during development. (A-D) In situ hybridization with Eya1 antisense probe. (E-H) In situ hybridization with TROY antisense probe. In all pictures, dorsal is up and rostral is to the left.

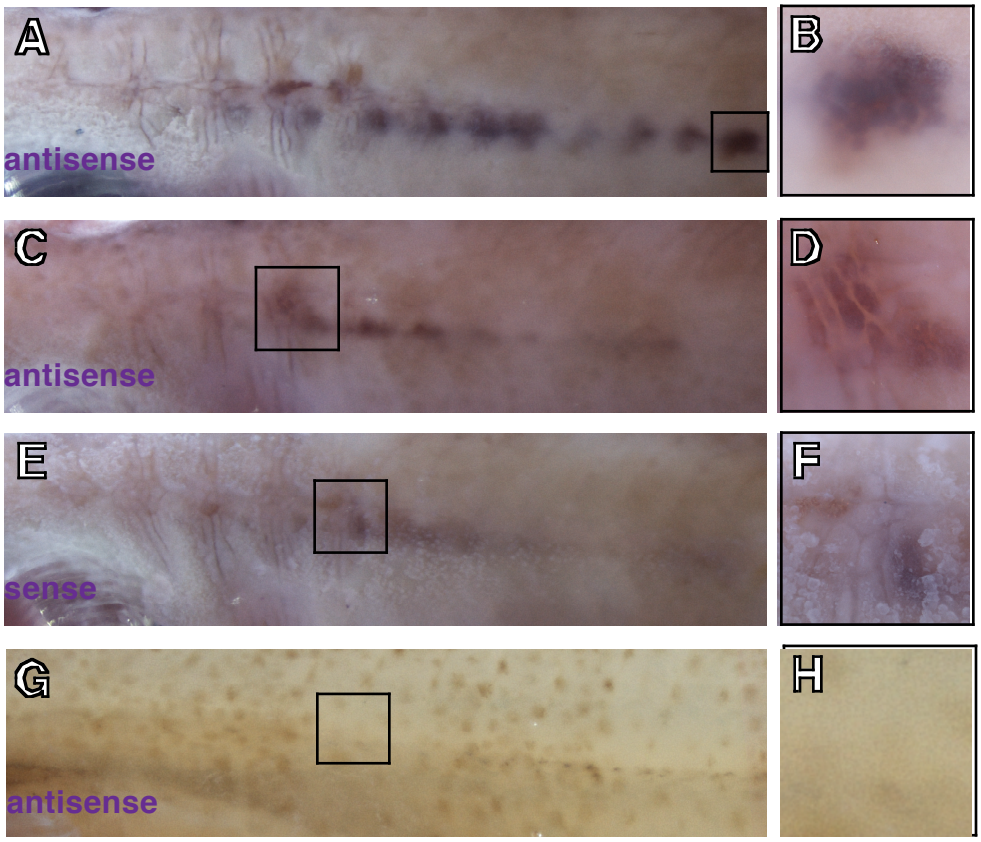

Figure 3-3. The novel gene ENSGACG00000002373 may be expressed near the lateral line in JP fish but not PB fish at 4wph.
(A-D) In situ hybridization with antisense probe for novel gene ENSGACG00000002373 on the flanks of two different JP fish. B and D are enlargements of the boxed areas in A and C. (E-F) In situ hybridization with sense probe for novel gene ENSGACG00000002373 on the flank of a JP fish. F is the enlargement of boxed area in E. (G-H) In situ hybridization with antisense probe for for novel gene ENSGACG00000002373 on the flank of a PB fish at 4wph. H is the enlargement of boxed area in G. In all pictures, dorsal is up and rostral is to the left.

Table 3-1. Differential expression of genes and alleles within the Chr XXI QTL as measured by RNA-seq on trunk RNA.

				Differential Expression			Allele-specific expression	
				Average RPKM				
Age	Gene	Location (Mb)	Ensembl gene ID	JP	PB	Fold difference (JP/PB)	No. of SNPs	Fold difference (JP/PB)
2wph	***CMBL***	**6.01**	**ENSGACG00000002636**	**9.9 ± 1.6**	**2.1 ± 0.2**	**4.8****	**5**	**4.64 ± 0.02**
	novel gene	7.26	ENSGACG00000003090	1.7 ± 0.4	5.4 ± 0.2	-3.1	0	-
4wph	*novel gene*	4.31	ENSGACG00000002362	10.6 ± 0.4	5.9 ± 0.3	1.8**	3	1.01 ± 0.07
	novel gene	**4.34**	**ENSGACG00000002373**	**10.56 ± 0.08**	**5.5 ± 0.4**	**1.9***	**4**	**2.56 ± 0.03**
	ZFHX4	4.92	ENSGACG00000002418	5.7 ± 0.2	2.98 ± 0.01	1.9**	20	1.05 ± 0.02
	HNF4G	5.12	ENSGACG00000002422	3.8 ± 0.7	5.3 ± 0.5	-1.4	4	1.7 ± 0.1
	novel gene	**5.18**	**ENSGACG00000002443**	**8.2 ± 0.4**	**3.1 ± 0.4**	**2.6****	**2**	**3.0 ± 0.3**
	novel gene	5.56	ENSGACG00000002475	99.8 ± 3.8	134.4 ± 0.8	-1.3**	3	-1.76 ± 0.04
	C8G	5.57	ENSGACG00000002477	54.4 ± 0.4	25.8 ± 0.8	2.1**	5	-1.06 ± 0.06
	MSRB2	**5.57**	**ENSGACG00000002478**	**13.2 ± 0.3**	**1.5 ± 0.6**	**8.7****	**4**	**5.29 ± 0.04**
	SHARPIN	**5.79**	**ENSGACG00000002544**	**9.3 ± 0.2**	**12.2 ± 0.6**	**-1.3**	**24**	**-1.48 ± 0.03**
	novel gene	5.80	ENSGACG00000002549	3.7 ± 0.1	6.2 ± 1.0	-1.7*	3	-1.96 ± 0.05
	novel gene	5.98	ENSGACG00000002620	61.6 ± 1.1	22.2 ± 0.8	2.8**	9	-1.20 ± 0.05
	CMBL	**6.01**	**ENSGACG00000002636**	**8.1 ± 0.1**	**3.4 ± 0.2**	**2.4****	**5**	**3.26 ± 0.02**
	NCOA2	6.91	ENSGACG00000002822	5.1 ± 0.2	3.03 ± 0.04	1.7	16	1.10 ± 0.02
	novel gene	7.26	ENSGACG00000002918	8.0 ± 0.8	19.4 ± 4.1	-2.4**	2	5.00 ± 0
	novel gene	7.26	ENSGACG00000003094	1.90 ± 0.05	3.4 ± 0.3	-1.8	0	-
	novel gene	7.26	ENSGACG00000003090	1.4 ± 0.3	2.6 ± 0.6	-1.9	0	-
	ATP8A2	7.64	ENSGACG00000003172	12.01 ± 0.02	7.3 ± 0.1	1.6	1	-1.3 ± 1.3

Genes identified by RNA-seq as being differentially expressed between JP and PB (adj. $p \leq 0.01$) at either 2wph or 4wph. * $p < 0.001$; ** $p < 0.0001$. RPKM was calculated by dividing number of reads for each gene by the Ensembl-predicted length for the gene and then by the total number of reads for that RNA-seq pool; Average RPKM is the mean for the two pools from each population at each age. Fold differences are the larger value divided by the smaller value; positive numbers indicate that the JP value is higher and negative numbers indicate that the PB value is higher. Numbers are plus or minus standard error. Bold text indicates genes selected for confirmation with qPCR and/or pyrosequencing (see **Table 3-2**).

Table 3-2. Differential expression of candidate genes within the Chr XXI QTL as measured by qPCR and pyrosequencing on trunk RNA.

			Differential Expression						Allele-specific expression	
			2wph			4wph				
Gene	Location (Mb)	Ensembl Gene ID	JP	PB	Fold diff. (JP/PB)	JP	PB	Fold diff. (JP/PB)	Fold diff. (JP/BP) 2wph	Fold diff. (JP/PB) 4wph
BMP6	3.83	ENSGACG00000002307	13.7 ± 1.3	15.3 ± 0.9	-1.1	2.6 ± 0.3	2.7 ± 0.1	1.0	-	-
TFAP2A	4.26	ENSGACG00000002334	684 ± 65	923 ± 64	-1.3	27 ± 3	14 ± 2	1.9*	-	-
novel gene	**4.34**	**ENSGACG00000002373**	**3.0 ± 0.3**	**1.6 ± 0.1**	**1.9****	**4.6 ± 0.2**	**2.0 ± 0.1**	**2.4****	**3.0 ± 0.03****	**3.2 ± 0.03****
novel gene[1]	5.18	ENSGACG00000002443	-	-	-	-	-	-	1.1 ± 0.02	1.1 ± 0.02
MSRB2	**5.57**	**ENSGACG00000002478**	**1.5 ± 0.1**	**0.99 ± 0.06**	**1.6**	**2.13 ± 0.08**	**0.29 ± 0.02**	**7.4****	**2.4 ± 0.05****	**3.0 ± 0.05****
SHARPIN	**5.79**	**ENSGACG00000002544**	**741 ± 90**	**575 ± 34**	**1.3**	**43 ± 2**	**57 ± 3**	**-1.3***	-	-
CMBL	**6.01**	**ENSGACG00000002636**	**8.6 ± 1.1**	**2.0 ± 0.2**	**4.2****	**7.2 ± 0.7**	**2.9 ± 0.2**	**2.5****	**4.2 ± 0.06****	**2.5 ± 0.08****
SEMA5A	6.07	ENSGACG00000002670	16.7 ± 0.5	21.1 ± 2.1	-1.3	8.4 ± 0.8	5.7 ± 0.4	1.5	-	-
CBLN2	6.29	ENSGACG00000002693	25 ± 3	26 ± 2	-1.1	0.40 ± 0.05	0.40 ± 0.04	1.0	-	-
SOCS6[2]	6.40	ENSGACG00000002698	17 ± 2	180 ± 28	-10.5**	0.10 ± 0.01	0.80 ± 0.04	-7.9**	-1.1 ± 0.02	-1.1 ± 0.03
TRPA1	6.76	ENSGACG00000002794	0.044 ± 0.004	0.05 ± 0.01	-1.2	0.023 ± 0.002	0.024 ± 0.001	-1.1	-	-
Eya1	**6.83**	**ENSGACG00000002803**	**210 ± 23**	**188 ± 14**	**1.1**	**28 ± 2**	**34 ± 2**	**-1.2**	**-1.3 ± 0.02****	**-1.4 ± 0.02****
CPA6[2]	7.18	ENSGACG00000002857	89 ± 5	209 ± 24	-2.3**	14 ± 1	21 ± 1.5	-1.5*	1.2 ± 0.03	2.1 ± 0.01**

Genes were selected for analysis by qPCR and pyrosequencing either because of their differential expression in RNA-seq (see **Table 3-1**) or because of their predicted function. Differential expression levels given are percentages of the reference gene *HPRT*. Fold differences are the larger value divided by the smaller value; positive numbers indicate that the JP value is higher and negative numbers indicate that the PB value is higher. Numbers are plus or minus standard error. Bold text indicates genes selected for analysis in skin-only RNA (see **Table 3-3**). For qPCR results, significance was determined by two-tailed t-tests, with Bonferroni correction for 26 pairwise comparisons: * $p < 0.002$; ** $p < 0.0001$. For pyrosequencing results, significance was determined by Mann-Whitney U Tests, with Bonferroni correction for 14 pairwise comparisons: * $p < 0.004$; ** $p < 0.0001$. [1]The novel gene ENSGACG00000002443 was only tested by pyrosequencing because no suitable qPCR primers could be found. [2]*SOCS6* and *CPA6* qPCR results were skewed by SNPs within qPCR primer sequences in JP fish.

Table 3-3. Differential expression of candidate genes within the Chr XXI QTL as measured by qPCR on skin RNA.

Gene	Location (Mb)	Ensembl Gene ID	2wph			4wph			Fold difference (trunk/skin)
			JP	PB	Fold diff. (JP/PB)	JP	PB	Fold diff. (JP/PB)	
novel gene	4.34	ENSGACG00000002373	6.5 ± 0.4	4.6 ± 0.3	1.4*	5.8 ± 0.3	2.5 ± 0.4	2.3**	1.9*
MSRB2	5.57	ENSGACG00000002478	9.5 ± 0.4	7.5 ± 0.6	1.3	10.9 ± 0.6	7.2 ± 0.8	1.5*	208**
SHARPIN	5.79	ENSGACG00000002544	21 ± 1	19.3 ± 0.7	1.1	23.8 ± 0.8	22.3 ± 0.9	1.1	1.3
CMBL	6.01	ENSGACG00000002636	0.7 ± 0.2	2.9 ± 0.2	-4.3**	0.5 ± 0.1	1.9 ± 0.3	-3.4*	5.0**
Eya1	6.83	ENSGACG00000002803	17 ± 1	17.8 ± 0.7	-1.1	14.7 ± 0.4	11.6 ± 0.9	1.2*	2.1*

Genes that showed allele-specific differential expression in trunk RNA (see **Table 3-2**) were examined for differential expression in skin RNA. Expression levels given are percentages of the reference gene HPRT. Fold differences are the larger value divided by the smaller value; positive numbers indicate that the JP value is higher and negative numbers indicate that the PB value is higher. In the comparison of expression in trunk vs. skin, expression is higher for trunk samples in all these cases. Numbers are plus or minus standard error. For skin qPCR results, significance was determined by two-tailed t-tests, with Bonferroni correction for 10 pairwise comparisons: * $P < 0.005$; ** $P < 0.0001$. For trunk/skin comparisons, significance was determined by two-tailed t-tests, with Bonferroni correction for 5 pairwise comparisons: * $P < 0.01$; ** $P < 0.0001$.

Chapter 4 – Pleiotropic effects of a single gene on skeletal development and sensory system patterning in sticklebacks

1. Introduction

Adaptation to a new environment often requires changes in numerous phenotypic traits [102-104]. Mechanisms that lead to the co-inheritance of suites of phenotypes might therefore facilitate adaptation [105-107]. Indeed, in many cases of adaptation to divergent habitats, experimental evidence demonstrates that multiple phenotypic traits map to the same genomic regions [108-116]. However, whether linked phenotypes are caused by variation in the same gene (i.e. pleiotropy) or in tightly linked genes is largely unknown because identification and experimental manipulation of the gene(s) is usually required [117-119]. The extensive phenotypic diversification of threespine sticklebacks in freshwater provides a tractable system to address this question [120].

A previous QTL mapping study of variation in the lateral line between JP and PB sticklebacks uncovered tight genetic linkage between neuromast patterning and lateral plate presence in the Mp line [69]. The presence of plates was strongly associated with the dorso-ventral arrangement of neuromasts in F2 hybrids, and both the number of plates and neuromast patterning in Mp (but not Ma) mapped to a region of Chr IV containing the gene *Ectodysplasin* (*Eda*). Using transgenic methods, this gene was previously shown

to be responsible for the difference in plate number between complete and low-plated sticklebacks [94]. This chapter focuses on dissecting the relationship between lateral plates, neuromast patterning in the Mp line, and the pleiotropic effects of *Eda* on both of these phenotypes.

2. Results and Discussion

A. Developmental correlation between lateral plate formation and neuromast patterning

To examine whether there was a developmental correlation between the formation of the lateral plates and the patterning of neuromasts, repeated calcein staining was used to follow plate formation across the development of individual fish from a completely-plated marine population (JP). Plate formation in this population follows the pattern described previously [121]. The first plates calcify near the Ma/Mp boundary (**Figure 4-1a**); additional plates are then added rostrally and caudally (**Figure 4-1b**). A second set of plates begins to calcify near the caudal fin (**Figure 4-1c**), and additional plates are then added to each set of plates until they join in the middle into a continuous series of plates (**Figure 4-1d**).

To then determine whether the patterning of neuromasts along the flank is associated with the development of the lateral plates, calcein and DASPEI co-staining was used to

track the temporal correlation between plate formation and neuromast location in two completely plated marine populations, JP and MC (Manchester Clam Bay, Washington). At hatching, fry from both populations have roughly one neuromast per body segment down the length of the trunk (**Figure 4-1e**). Developing plates begin to calcify directly around the single neuromast in that segment (**Figure 4-1f**). As the plates grow in height, additional neuromasts appear above and below the original neuromast (**Figure 4-1g**). As the plates near the caudal fin begin to calcify, the same process is repeated in those segments (**Figure 4-1h**). Eventually, the two nascent neuromasts in each segment remain, while the primary neuromast is no longer visible (**Figure 4-1i**).

While each fish appears to follow this general schedule of plate development and neuromast pattern elaboration, the size of the fish at the beginning of plate formation and the exact order of plate addition do not appear to be highly stereotyped (**Figure 4-1j**). Within each fish, however, the correlation between plate addition and neuromast pattern through development is striking, as can be seen in a segment-by-segment overlay of plate presence and neuromast arrangement across MC fish of a variety of sizes (**Figure 4-1j**). Specifically, in developing MC fish, the presence of a plate in Mp is strongly associated with a dorso-ventral arrangement of neuromasts within that segment. The vast majority of unplated segments in Mp possess neuromasts located along the midline, whereas neuromasts in plated Mp segments are significantly more likely to be located off of the midline (**Table 4-1;** Fisher's exact test, $p<0.0001$). Given the tight spatial correlation

between the appearance of the primary neuromast and the beginning of plate calcification, it is tempting to speculate that neuromasts provide a location cue for plate formation, as has been hypothesized for dermal bones in the heads of other fishes (see [55, 122] for reviews). Testing this hypothesis will require the identification of plate precursor cells, as well as development of a method for ablating neuromasts that leaves those plate precursor cells intact: mechanical ablation of the lateral line primordium prior to its migration was suggested by de Beer [123] as a way to test the necessity of neuromasts to bone formation, but without prior identification of the plate precursor cells, there remains the chance (however slim) that ablation of the lateral line primordium would also disrupt the plate precursor cells themselves directly.

B. Transgenic expression of *Eda* reveals pleiotropic effects on lateral plate formation and neuromast patterning

The developmental analysis thus revealed a close relationship between plate formation and neuromast patterning. Previous work in the Peichel lab has shown strong phenotypic correlations between lateral plate presence and lateral line patterns observed across complete- and low-plated populations [58] as well as in genetic crosses [69]. Together, these findings led to the hypothesis that *Eda* has a pleiotropic effect on both phenotypes. To test this hypothesis, *Eda* expression was manipulated with transgenesis to drive ectopic plate formation in low-plated sticklebacks. The completely-plated (JP) *Eda* allele is dominant to the low-plated (PB) *Eda* allele for plate formation [80, 94], and *Eda*

expression is 1.7-fold higher in JP fish than in PB fish once plate calcification begins (relative expression JP: 0.96 ± 0.09 (n=12); PB: 0.57 ± 0.05 (n=12); Kruskal-Wallis $\chi^2(1)= 9.3$; $p<0.0025$). Thus, the human cytomegalovirus (CMV) promoter was used to upregulate *Eda* expression in PB fish. Injection of the CMV:*Eda* transgene into PB embryos caused formation of ectopic plates in both Ma and Mp (**Figure 4-2b**); the focus here is on Mp because the pattern of neuromasts in Mp (but not Ma) is linked to *Eda* [69]. Transgene-injected mosaic fish had significantly more plates in Mp than their uninjected siblings (transgene-injected fish: 3.1 ± 0.6 (n = 19); uninjected controls: 0.05 ± 0.05 (n = 21); Kruskal-Wallis $\chi^2(1)= 19$; $p<0.0001$). Transgene-injected fish also had significantly more segments in Mp that had dorso-ventral neuromasts (percentage of total segments with dorso-ventral neuromasts in transgene-injected fish: 7.7% (n = 11); uninjected controls: 0.3% (n = 13); Kruskal-Wallis $\chi^2(1) = 22$, $p<0.0001$). This shift in patterning was strongly associated with the presence of ectopic plates (**Figure 4-2a,b; Table 4-2;** Fisher's exact test, $p<0.0001$). In transgene-injected fish, neuromasts were located dorsal and/or ventral to the midline in 44.4% of the segments with ectopic Mp plates, but in only 0.4% of unplated Mp segments. This result reveals that *Eda* has pleiotropic effects on both neuromast patterning and plate development.

Although these results demonstrate that transgenic expression of *Eda* in the PB background does lead both to ectopic plate formation and to changes in neuromast patterning, there are relatively few ectopic plates in the Mp line of PB transgene-injected

fish and not all of these plates have a dorsal-ventral arrangement of neuromasts. These findings are consistent with previous results demonstrating that interactions between *Eda* and modifier loci in the PB background influence both plate number [80] and neuromast pattern [69]. To determine whether these modifiers were also affecting the *Eda* transgene, the CMV:*Eda* transgene was expressed in a second low-plated background: low-plated PBxJP F3 hybrids. These hybrids were verified to be homozygous for PB alleles in at least a 7 Mb region around *Eda,* but should have an assortment of PB and JP alleles at other plate modifier loci. In this F3 hybrid background, the average number of plates in Mp increased dramatically, from 0.4 ± 0.1 in uninjected controls (n = 26) to 12 ± 3 in transgene-injected fish (n = 12) (Kruskal-Wallis $\chi^2(1) = 18$, $p<0.001$). This was a significantly higher number of ectopic Mp plates than that observed in PB transgene-injected fish (**Table 4-2**; Kruskal-Wallis $\chi^2(1) = 6.2$, $p<0.05$). In F3 hybrids, the *Eda* transgene also significantly increased the number of Mp segments with a dorso-ventral arrangement of neuromasts (percentage of total segments with dorso-ventral neuromasts in uninjected controls: 1.5% (n = 15); transgene-injected fish: 50.7% (n = 12); Kruskal-Wallis $\chi^2(1) = 191$, $p<0.0001$). Similar to the effect of the *Eda* transgene in the PB background, the significant shift in the distribution of neuromasts was strongly linked to being located on plates (**Figure 4-2c,d,e; Table 4-2;** Fisher's exact test, $p<0.0001$). However, compared with the pure PB background, a significantly higher proportion of these ectopic plates had vertically-arranged neuromasts in F3 hybrids: neuromasts were located dorsal and/or ventral to the midline on 95% of ectopic Mp plates in F3 mosaic

fish *vs.* 44.4% in PB mosaic fish (**Table 4-2;** Kruskal-Wallis $\chi^2(1) = 51$, $p<0.0001$). These results support previous genetic mapping studies demonstrating that modifier loci contribute to differences in these phenotypes between the JP and PB populations [69, 80]. Additional genetic mapping and cloning experiments are required to determine whether the modifier loci act independently or have pleiotropic effects on the two phenotypes.

These independent transgenic experiments provide strong support for the conclusion that *Eda* has pleiotropic effects on both the development of the lateral plates and the patterning of the lateral line. There are two possible mechanisms to explain the pleiotropic effects of *Eda* on these two phenotypes. *Eda* could have a direct effect on neuromast patterning that is independent of its effect on plate development. Alternatively, *Eda* could have an indirect effect on neuromast patterning, which is mediated by its influence on plate development. At this point, we cannot distinguish between these alternatives. However, studies in medaka and zebrafish demonstrate that the presence of dermal bone affects the patterning of some neuromasts [124], suggesting that similar mechanisms might occur in sticklebacks. Testing these alternative mechanisms would require ablation of the lateral plate precursor cells without disruption of the neuromasts in a transgenic background.

While the molecular genetic basis of lateral plate variation is now well-described [73, 80, 94], the selective forces that generate this variation remains a subject of debate [74, 125].

Our results demonstrate that the repeated loss of lateral plates in freshwater stickleback populations is accompanied by a change in the lateral line sensory system. Thus, our work reveals that repeated selection for the low-plated *Eda* allele in freshwater could be the result of selection on the lateral line, rather than on lateral plates. Furthermore, many other phenotypes have been linked to the region around *Eda*, such as pelvic spine length [81], body shape [82, 126, 127], color [126], growth rate [128, 129], salinity preference [130], and schooling behavior [131], all of which could also be targets of selection. Although associations between *Eda* genotype and survival and fitness in freshwater have been previously demonstrated [128, 129, 132, 133], these experiments could not distinguish between the effects of *Eda* and linked loci. The transgenic fish generated for this study, and any stably transgenic lines obtained from them, will enable a rigorous analysis of the pleiotropic effects of *Eda* on both phenotypes and fitness. Determining which traits are caused by *Eda* itself or by other loci in tight linkage with *Eda* will enable future studies to determine both the agents and phenotypic targets of selection at this locus, thereby making key connections between genotype, phenotype and fitness [66].

A
11.0 mm
B
12.5 mm
C
14.2 mm
D
16.8 mm
E
F
G
H
I

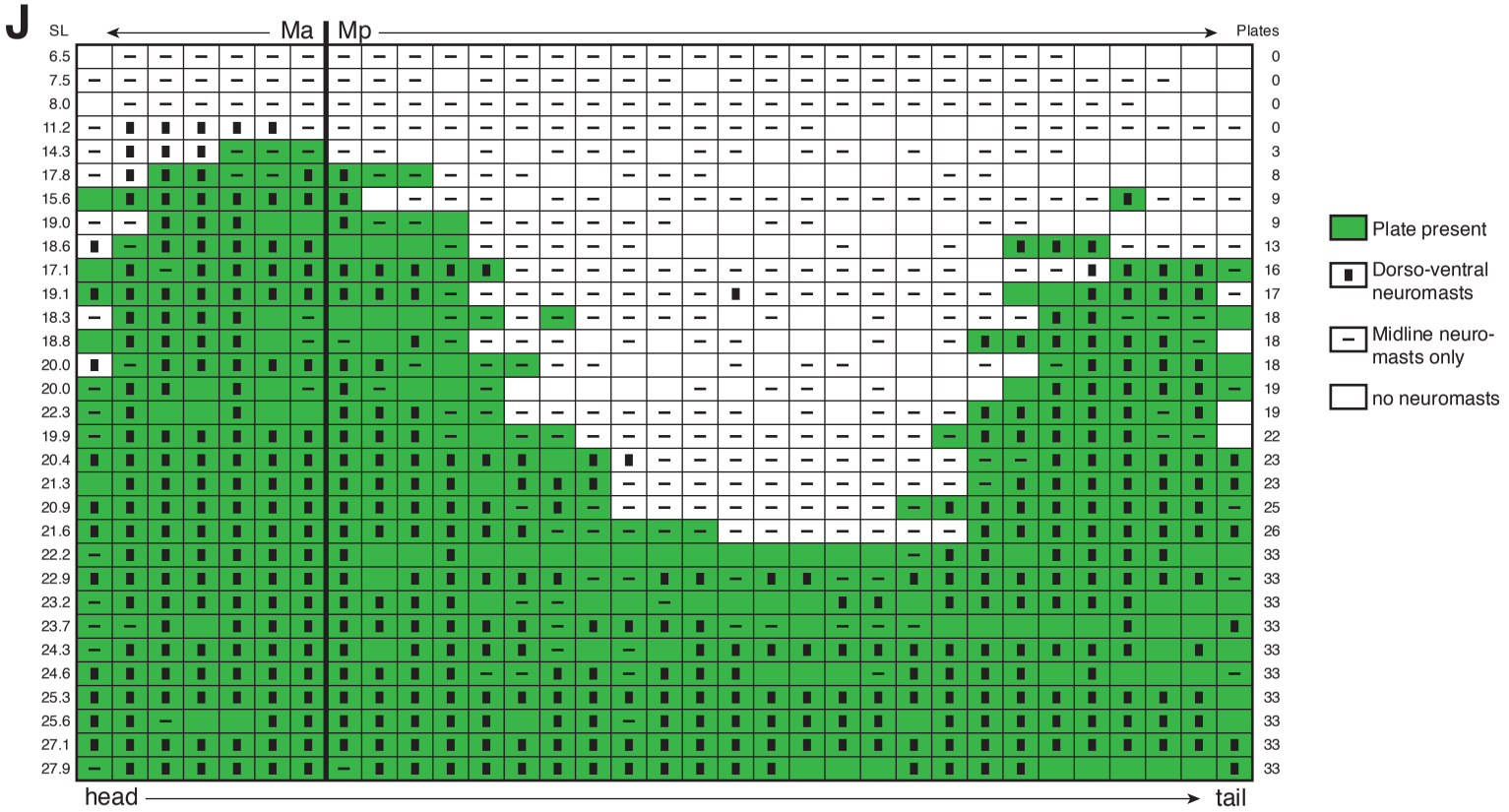

Figure 4-1. Bony plates and neuromast patterning are correlated through development in completely-plated fish.
(A-D) Bone development in a single JP fish, repeatedly stained with calcein during development. The standard length of the fish is indicated in mm. The near-vertical white line in D indicates the location of the boundary between the Ma and Mp lines. (E-I) Detail of neuromast and plate development along the posterior flank of DASPEI- and calcein-stained JP fish (scale bar = 0.1 mm); F-I match the boxed regions in A-D, although the pictures are from different fish. (J) Compilation of plate presence and neuromast pattern along the length of MC fish at a range of sizes, showing the correlation between plate development and neuromast pattern elaboration. Each horizontal row is a single individual fish; fish are sorted in order of total number of plates. The vertical line between columns seven and eight indicates the location of the boundary between the Ma and Mp lines. Green shading indicates the presence of a plate, white indicates no plate, an unfilled box indicates no neuromasts present, a horizontal line indicates neuromasts along the midline, a vertical box indicates dorso-ventral arrangement of neuromasts.

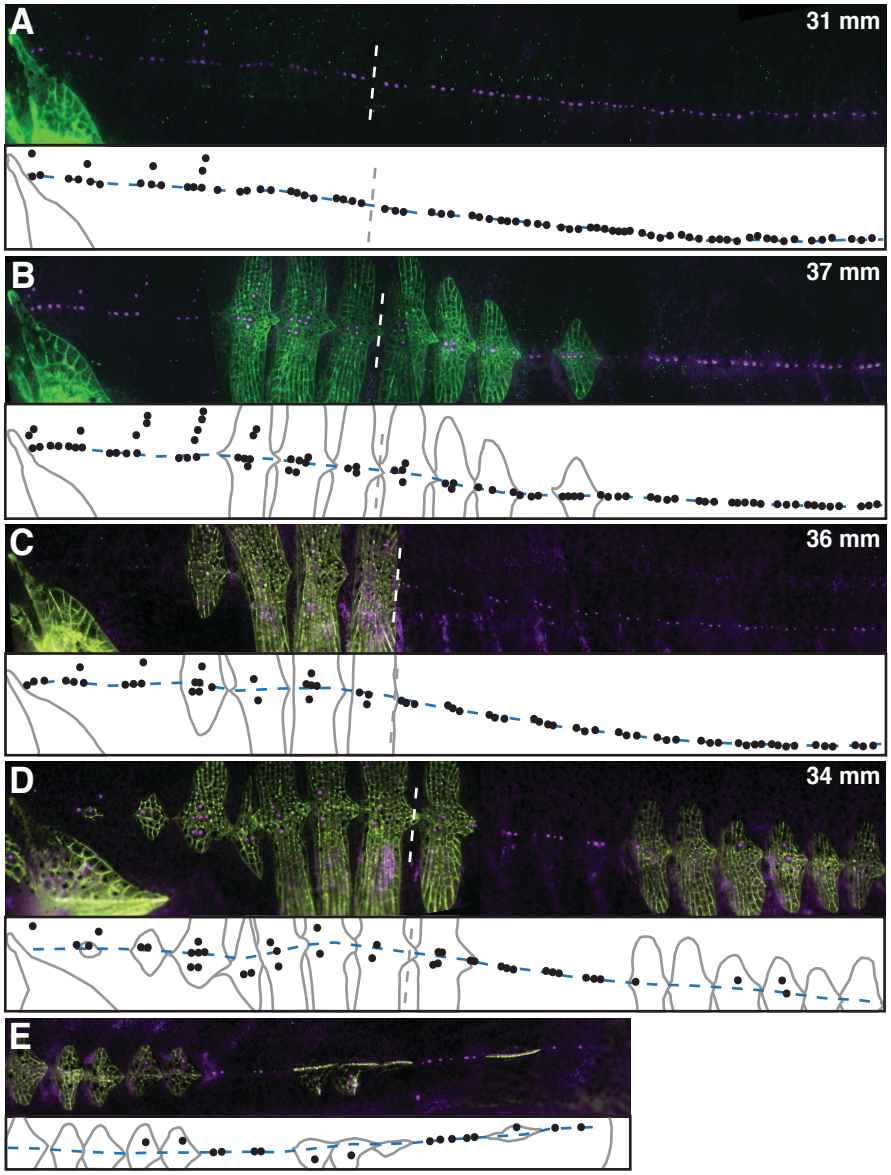

Figure 4-2. Transgenic expression of Eda increases number of plates and alters neuromast patterning. (A-E) Plates were visualized with calcein (green) and neuromasts were visualized with DASPEI (purple) on representative control and transgene-injected fish from PB and PBxJP low-plated F3 backgrounds, the Ma/Mp boundary is shown (white dotted line); schematics below each image show plate edges (grey lines), neuromast placement (black dots), Ma/Mp boundary (vertical or near-vertical grey dotted line) and the midline (blue dashed line). For all fish, dorsal is up and rostral is to the left, with the shoulder girdle (cleithrum) appearing to the left of the first Ma segment. The standard length of each fish is indicated in mm. (A) PB control; (B) PB transgene-injected mosaic; (C) PBxJP low-plated F3 control; (D) PBxJP low-plated F3 transgene-injected mosaic; (E) Remainder of the flank from the individual shown in (D). Individual frames comprising B were tilted slightly with respect to each other to correct for bend in fish body during photographing.

Table 4-1. Plate presence and neuromast pattern are correlated through development.

	dorso-ventral	midline
plate	289	72
no plate	3	272

Combined segment totals (average 25.5 segments per fish) for MC fry at a range of stages in plate development (n=31 fish).

Table 4-2. Transgenic sticklebacks demonstrate that *Eda* expression affects both plate presence and neuromast pattern.

		Transgenic		Control	
Population		dorso-ventral	midline	dorso-ventral	midline
PB	plate	20	25	1	0
	no plate	1	226	0	342
PBxJP F3	plate	114	6	5	0
	no plate	0	105	0	329

Combined segment totals (average 25.5 segments per fish) for transgenic and uninjected control siblings from both PB and PBxJP F3 backgrounds. PB: Transgenic n=11 fish, Control n=13 fish; PBxJP F3: Transgenic n=12 fish, Control n=15 fish.

Chapter 5 – Discussion

The lateral line is a popular system in which to study topics of general interest in developmental biology, like cell migration and differentiation, and the signaling events and molecules that underlie these processes [28, 29, 31]. The incredible array of lateral line patterns found in different species of fish, combined with the roles that the sensory capacity of the lateral line is thought to play in the lives of those species, also make the system an exciting subject of evolutionary study [54, 55, 134].

In my thesis research, I focused on various aspects of the development and evolution of the lateral line in threespine stickleback fish. First, I investigated the difference in neuromast number on the flanks of fish from marine and freshwater populations. Differences in the posterior trunk (Mp) line had been previously mapped to a QTL on Chr XXI. I attempted to narrow this region by adding additional markers and additional individuals to those previously used, and also by investigating the same phenotypic difference in a cross between different stickleback populations. To identify the gene(s) underlying the difference in neuromast number, I used several different molecular techniques as well as next generation sequencing, and identified a gene that may be the previously-described plate modifier locus on Chr XXI. Finally, I described the development of the neuromast arrangement in the Mp line and its correlation with the development of the bony plates. I used transgenic gene expression to demonstrate that the

Eda gene, previously identified as the gene responsible for plate formation in marine fish, was also responsible for the neuromast pattern phenotype. There are a number of remaining questions raised by my research about the development of the lateral line, the development of the lateral line in relation to associated bony plates in sticklebacks, and the evolution of both structures.

1. Developmental basis of an increase in Mp neuromasts

Several developmental questions were suggested by my work on the difference in neuromast numbers between stickleback populations, besides the primary question of the identity of the gene(s) that underlie the differences. First, where do the extra neuromasts of PB come from? In zebrafish, there are two ways in which neuromasts are added to the postembryonic lateral line: by differentiation of interneuromast cells laid down by the same primordia that deposited the initial neuromasts [50], or by budding from those existing neuromasts [40, 49, 124]. Because I was unable to reliably follow the development of the lateral line in a single fish, I could not distinguish between these two possibilities, although the answer has implications for the mechanism of action of the gene(s) responsible for the difference neuromast number, both in the PBxJP cross and in the HTxPB cross. Zebrafish neuromasts have been shown to increase in number by the removal of (presumably inhibitory) glia, which led to the increased differentiation of interneuromast cells [50, 51], but none of the genes in the QTL on Chr XXI had functions that were predicted to affect glial development or function.

Second, do stickleback neuromasts in the Mp line vary in polarity? This could be informative for the developmental origin of the additional neuromast in PB because neuromasts deposited by the two separate primordia that migrate along the zebrafish flank (called primI and primII) can be distinguished by their polarity [39], as revealed by phalloidin stain/acetylated tubulin antibody or by alkaline phosphatase staining [135]. This difference in polarity of neuromasts deposited by different primordia appears to be a general feature of lateral line development in fish [30] and amphibians [136]. This difference in polarity likely has effects on the sensitivity of the fish to water movement in different directions [137, 138]. Attempts to stain neuromasts from both JP and PB fish with either alkaline phosphatase or phalloidin stain/acetylated tubulin antibody to determine their orientation did not reveal any of the obvious polarity observed in zebrafish neuromasts (A. Greenwood and M. Dubin, pers. observation), but staining at earlier stages or observing the stained neuromasts under higher magnification might reveal the polarity and suggest a source for the supernumerary PB neuromasts.

2. Developmental relationships between lateral plates and lateral line patterning

My investigation of the relationship between lateral line pattern and dermal bony plates on the trunk of sticklebacks raised several developmental questions about the potential patterning interactions between these structures. First, are bony plates causing alteration to the arrangement of neuromasts? Neuromasts are often located dorsal or ventral to the

midline in the presence of a plate, and almost never located off the midline in the absence of a plate. The effect of dermal bones on neuromast patterning has been demonstrated in one case: Wada et al. [124] showed that in zebrafish the positions of the neuromasts over the opercle were influenced by the presence and growth of the opercle and subopercle bones themselves, with the neuromasts being carried along by migrating peridermis over the expanding edge of the bones. We showed that expression of the *Eda* gene was responsible for the difference in neuromast positioning as well as the difference in plates between marine (completely-plated) and freshwater (unplated) sticklebacks, but the mechanism for this remains to be elucidated. If the plates themselves are involved in altering neuromast pattern, there are two aspects of plate development that differ between PB and PBxJP F3 transgenic backgrounds that may indicate the reason so many fewer plated segments show dorso-ventral arrangement of neuromasts in PB fish (**Table 4-2**), and therefore may suggest the mechanism by which plate presence and neuromast arrangement are connected. First, the timing of plate formation may be responsible for the difference in transgenic phenotype. When re-phenotyping transgenic PB fish, we sometimes observed more plates than had been recorded on previous viewings, and we never saw this with PBxJP F3 transgenic fish (MM and A. Greenwood, pers. observation). This suggested that plate development started later or continued more slowly in PB fish than in PBxJP F3s. If plate development in the PB background was delayed, then neuromasts would not receive a signal to develop a dorso-ventral arrangement when they are competent to respond. This will need to be tested by

comparing the timing of plate development in stable PB transgenic fish to that in fish from completely-plated populations (nontransgenic PB fish are not informative because they almost never have plates in Mp, **Table 4-2**). Second, I noted that the ectopic plates were smaller in the PB transgenics than in the PBxJP F3 transgenics (MM, pers. observation), which is consistent with loci for plate size segregating in these populations as well [80]. This reduced plate size may mean that, even if plate development begins at an appropriate time, neuromasts do not receive a sufficient signal to develop the vertical arrangement of neuromasts. However, even small plates show dorso-ventral patterning in developing MC fish (**Figure 4-1j**). The "small-plated" sticklebacks from northern Europe [139] would provide another useful reference for this analysis, to see whether timing of plate development or size of plates is necessary to prompt the dorso-ventral pattern of neuromasts.

Second, do neuromasts affect the placement or development of bony plates? Ossification of the plate initiates immediately around the central neuromast within each segment. The effects of neuromasts on bony elements has been widely reported, although for the anterior (cranial) lateral line more than the posterior: in many fishes, ossification of the bones of the skull begins immediately around the neuromasts that will later occur in canals through those bones [55, 123, 140, 141]. There is much debate in the literature about whether the neuromasts cause ossification of dermal bones [55]. The argument against the necessity of neuromasts in this process is that there are bones that do not have

lateral line canals, and that therefore initiate ossification without the help of neuromasts. Just because neuromasts are not necessary in every case does not prove that they are unnecessary in all cases, however, either to initiate ossification directly or to provide a location cue for the ossification process. I attempted to ablate the neuromasts of developing stickleback fry using copper sulfate, which had been reported to permanently ablate neuromasts in zebrafish [142] (unlike the temporary ablations caused by exposure to aminoglycoside drugs), but I was unsuccessful: stickleback neuromasts regenerated promptly upon cessation of copper treatment, even at concentrations of copper just short of lethal for the fish (MM, pers. observation). Mechanical ablation of the premigratory lateral line primordia has been suggested as a means to test whether the neuromasts are necessary for dermal plate formation [123], but without identification of the plate precursors, it would be difficult to be sure the ablation of the primordium had not also affected the plate precursors directly.

3. Role of the *Eda* gene in lateral plate development and lateral line patterning

Eda was shown to be the primary gene underlying the striking difference in bony plate phenotypes between populations [94], but is the causative difference in *Eda* between complete- and low-plated populations coding or regulatory? The coding sequence of the *Eda* gene has been shown to differ between completely-plated and low-plated populations, along with the sequence of the surrounding region [94]. The mouse *Eda* gene was used by Colosimo *et al*. [94] to drive ectopic plates in low-plated sticklebacks,

which by itself argues that it is level of expression rather than coding sequence that is responsible for the difference in plate phenotype between complete and low-plated morphs. We showed that the *Eda* gene is more highly expressed in JP than in PB fish during plate development (see Chapter 4), which adds to the argument. But most conclusively, we used the same CMV promoter to overexpress the PB coding sequence of *Eda* in a low-plated fish and observed ectopic plates, demonstrating that even the PB allele of *Eda* is sufficient to drive plate formation if expressed at the right level. However, because that one CMV:PB-*Eda* fish died before I could look at its neuromasts, I cannot rule out a role for the coding sequence of *Eda* in affecting neuromast position.

Through which receptor does *Eda* act on plates and neuromasts? In mice, the A1 splice form of the *Eda* ligand signals through *EDA Rece*ptor (*EDAR*) in the formation of skin appendages (hair follicles and sweat glands) [143], while in medaka fish, mutation of the *Edar* gene results in a lack of scales (a skin appendage of a different kind) [144, 145]. Mutations in the *Eda* signaling pathway are well-known in humans, and most occur in the X-linked *Eda* gene itself, with most of the rest occurring in the autosomal genes *EDAR* and *EDAR-Associated Death Domain* (*EDARADD*), affecting the development of teeth and other exocrine glands in addition to hair follicles and sweat glands [146]. In sticklebacks, the Eda ligand has two potential receptors, EDAR and TROY [93]. I confirmed earlier *in situ* hybridization results from our lab, showing that *TROY* is expressed in the immediate vicinity of the lateral line during development, in or around

all neuromasts and interneuromast cells. This makes TROY an intriguing candidate for the receptor to mediate the effect of Eda on lateral line patterning, and all the more intriguing if it mediates Eda's effects on neuromast phenotype without affecting plate phenotype. Knockdown of *TROY* in either completely-plated fish or PB fish that are transgenic for *Eda* overexpression, perhaps using TALENs [147], would allow confirmation of this hypothesis.

4. Evolution of the stickleback lateral line

For each of the outstanding questions about the development of the lateral line in sticklebacks, there is also a question about the evolutionary pressures that have shaped the processes I observed. Why do PB fish have so many more neuromasts than fish from other populations? Why do neuromasts exhibit a dorso-ventral arrangement in some populations and not in others? Why do threespine sticklebacks lack canal neuromasts, in contrast to the related ninespine stickleback [85]? Webb [55] offers several reasons for observed variation in lateral line morphology: the differing patterns may be the result of adaptation, either to flow regime or behavior; or they may be the result of phylogenetic or developmental constraints. The threespine stickleback is a useful model in which to address the adaptive value of lateral line phenotype, because of the wealth of natural history information available [70]. Marine and freshwater sticklebacks may exhibit different arrangements of neuromasts in their posterior lateral lines because the neuromast pattern is constrained by the plate phenotype in each environment.

Alternatively, *Eda* genotype and plate phenotype may be selected for because of the effect they have on the lateral line (i.e., because of the difference in arrangement of neuromasts or because of the way in which the bony plates alter or filter the water flow experienced by the neuromasts associated with them) rather than because of any specific advantage or disadvantage of the plates themselves. Or, both plate and lateral line phenotypes may be selected for because of a pleiotropic effect of *Eda* on another phenotype or because of a phenotype caused by a separate tightly-linked gene. The frequency of *Eda* alleles within a population can change rapidly [148], demonstrating that selection on the locus continues to be important for stickleback evolution.

Sticklebacks are also a tractable behavioral model [149-151], so it may be possible to address the functional effect of variation in lateral line pattern on the way in which different fish experience their environments. Do the extra neuromasts in PB fish enable them to detect their benthic prey? Do dorso-ventral neuromast arrangements make it easier to maintain body position in a school? Manual ablation can be used to temporarily alter the number or arrangement of neuromasts in the lateral line. Experiments testing neuromast-ablated fish in the model school assay [151] or prey-capture assays (some of which are ongoing) may answer these questions about the utility of different lateral line patterns. Fish with permanent alterations to neuromast phenotype, like those transgenic fish generated in my research, could be used in experimental ponds [128] to directly test the fitness of fish with various combinations of genotypes and phenotypes.

5. Conclusion

Studies that combine developmental and evolutionary approaches to the lateral line have only recently been done [48, 53, 134]. However, the lateral line is an exciting system to study in sticklebacks and other species as a means to connect genetic and developmental changes with behavioral changes that are relevant for adaptation in the wild.

Chapter 6 – Methods

1. Fish care

All animal protocols were approved by the Fred Hutchinson Cancer Research Center Institutional Care and Use Committee (protocol #1575). All sticklebacks were lab-reared from *in vitro* crosses of fish from Manchester Clam Bay, Washington (MC), Akkeshi, Japan (JP), Paxton Lake benthic, British Columbia (PB), and Humptulips Pond, Washington (HT) populations. Fish were housed in 29-gallon glass aquaria with independent filtration and air stone aeration. Water in each tank contained 3.5 g/L Instant Ocean salts (Instant Ocean, Cincinnati, OH) and 0.4 g/L $NaHCO_3$. The fish were kept at summer conditions of 15.5°C on a 16h/8h light/dark cycle. Eggs and fry were contained in net breeders suspended from the side of the tank until 2 weeks after hatching. Young fish were fed *Artemia* nauplii twice daily, and adults were fed *Artemia* nauplii and frozen *Mysis* shrimp.

2. Mapping crosses and genotyping

An F2 intercross for genetic mapping, generated from a cross between a PB female and a JP male, was described previously [69]. Additional fish from these F2 families, particularly recombinants within the QTL previously identified on Chr XXI, were identified as follows: fish from additional F2 families from the same founder crossed were anesthetized, fin clipped, and returned to tanks in groups of four to eight fish. DNA

from these fin samples was genotyped at four microsatellite markers as described below: 4.5 Mb, 5.7 Mb, 7.9 Mb, and 8.5 Mb. Any tank in which we identified a fish that was recombinant between the markers at 5.7 Mb and 7.9 Mb (had PB alleles at 4.5 Mb and 5.7 Mb but JP alleles at 7.9 Mb and 8.5 Mb, or vice versa) was marked for retesting, and all fish in that tank (recombinant or not) were individually phenotyped and re-genotyped throughout the region of interest on Chr XXI as described below.

A second F2 mapping population was generated by crossing a single wild-caught HT female to a single lab-raised PB male to generate an HTxPB F1 cross. Fish from this F1 family were crossed to each other to generate three F2 families.

Genomic DNA was isolated from caudal fin tissue using Proteinase K/SDS digestion, followed by phenol/chloroform extraction. PBxJP F2 individuals (234 from the previous study [69] and 40 new) were genotyped at 10 microsatellite markers across the first half of Chr XXI; 0.8 Megabases (Mb) (Stn222, [75]), 4.0 Mb, 4.5 MB, 5.7 Mb, 6.8 Mb, 7.2 Mb, 7.9 Mb, 8.5 Mb, 9.0 Mb, and 9.5 Mb. HTxPB F2s were genotyped at 6 microsatellite markers: 0.8 Mb (Stn222), 4.5 Mb, 5.7 Mb, 6.8 Mb, 7.9 Mb, and 8.5 Mb. Microsatellite marker identities, locations, and primer sequences are given in **Table 6-1**. Primers were designed using Primer3 [152, 153] and forward primers were labeled with one of three 5' fluorescent conjugates: 6FAM (blue), VIC (green), or NED (yellow). Labeled PCR fragments were run on an ABI3730xl sequencer (Applied Biosystems/Life Technologies,

Carlsbad, CA) and fragment sizes were analyzed with GeneMapper (Applied Biosystems, Carlsbad, CA). JoinMap 3.0 (Kyazma, Netherlands) was used to construct a linkage map for each cross using the microsatellite markers listed above (using only the original 234 fish from the PBxJP F2 cross, to avoid skewing the map by incorporation of extra recombinants). MapQTL 4.0 (Kyazma, Netherlands) was used to compute likelihood of odds (LOD) scores for the association between genotype and phenotype at each marker.

3. Imaging of neuromasts and lateral plates

To visualize neuromasts, live fish were placed in 0.025% 2-(4-(dimethylamino)styryl)-N-ethylyridinium (DASPEI; Invitrogen/Molecular Probes, Carlsbad, CA) in embryo medium for 15 minutes, rinsed with clean embryo medium (1 mM $MgSO_4$, 120 μM KH_2PO_4, 74μM Na_2HPO_4, 1 mM $CaCl_2$, 500 μM KCl, 15 μM NaCl, 500 μM $NaHCO_3$), then anesthetized with fresh 0.013% MS-222 (Finquel tricaine methanesulfonate; Argent Chemical Laboratories, Redmond, WA) in embryo medium, adjusted to pH 7.2 with NaOH (Fisher Scientific, Pittsburgh, PA). To visualize calcified bone, live fish were placed in 0.2% calcein (Sigma-Aldrich, St. Louis, MO) in embryo medium for 10 minutes, washed twice with clean embryo medium, then anesthetized as after DASPEI staining. For costaining with calcein and DASPEI, fish were stained first with calcein, returned to their tanks, and then stained with DASPEI one to two days later.

To describe the developmental processes by which the adult lateral line pattern is produced in completely-plated populations, clutches of marine (JP and MC) fish were followed through development. Repeated calcein staining was performed in JP fish to characterize patterns of plate formation in individuals. Fish used for repeated imaging were kept in individual plastic cups starting at one week post hatching, in 100 ml of zebrafish embryo medium that was changed daily. For approximately two months they were stained once a week with calcein, lightly anesthetized, photographed under the microscope, and returned to their cups.

Unfortunately, repeated DASPEI staining could not be performed to visualize neuromasts on the same individuals because this leads to a loss of reliable neuromast staining over time (MM, pers. observation). Thus, we also stained unique fish simultaneously with DASPEI and calcein at a range of sizes after hatching. Plate and neuromast phenotypes were scored as follows: within each body segment, any calcein-stained bone (including the first sliver to appear around the central neuromast, **Figure 4-1f)** was scored as a plate; segments were scored as "dorso-ventral" if they contained any neuromasts above or below the midline, "midline" if they contained neuromasts located exclusively on the midline. The midline of neuromast placement was determined based on the midline ridge of plates (in plated segments) or in relation to the surrounding neuromasts (in unplated segments).

All microscopy was performed using a Nikon Eclipse 80i microscope (Nikon Instruments Inc., Melville, NY) with FITC/Texas Red filter cubes and manual stage and focus. Images were recorded using a Photometrics Cool-snap ES2 camera (Photometrics, Tucson, AZ), then pseudocolored and uniformly enhanced for brightness and contrast with NIS-Elements imaging software (Nikon Instruments Inc., Melville, NY). Composite (whole body and whole flank) pictures were stitched together using Adobe Photoshop.

4. RNA isolation and deep sequencing

Tissue samples were collected from developing PB, JP, and PBxJP F1 fry at 2 weeks post-hatching (~12 mm standard length, when both parental populations have one neuromast per segment in Mp) and 4 weeks post-hatching (~17 mm standard length, when the difference in neuromast phenotype between the populations has begun to appear). RNA was isolated separately from 12 individuals from each population at each age in TRIzol (Invitrogen, Carlsbad, CA). Two different tissue sources were used: whole trunk (all tissue posterior to the operculum, with tissue disrupted using an immersion homogenizer) and skin (peeled off with some underlying muscle) from between the second dorsal spine and the caudal peduncle, with tissue disrupted using a 5mm stainless steel beads in a TissueLyzer, Qiagen, Venlo, Netherlands).

RNA-seq libraries were prepared from trunk total RNA (two pools per age per population, with 6 individuals in each pool) using the TruSeq RNA Sample Prep Kit v2

(Illumina, Inc., San Diego, CA, USA). Library size distributions were validated using an Agilent 2100 Bioanalyzer (Agilent Technologies, Santa Clara, CA, USA). Additional library quality control, blending of pooled indexed libraries, and cluster optimization were performed using Agilent Technologies' QPCR NGS Library Quantization Kit (Agilent Technologies, Santa Clara, CA, USA). RNA-Seq libraries were pooled and clustered onto a flow cell lane using an Illumina cBot. Sequencing was performed on an Illumina HiSeq 2000 using a paired end, 50 base read length (PE50) sequencing strategy. Image analysis and base calling were performed using Illumina's Real Time Analysis v1.13 software, followed by 'demultiplexing' of indexed reads and generation of FASTQ files, using Illumina's CASAVA v1.8.2 software. Only reads that passed the default chastity threshold (≥ 0.6) were used in downstream analyses.

Reads from each pool were aligned to the *Gasterosteus aculeatus* reference genome (BROADS1.66 assembly) using TopHat [90], with an expected inner distance between mate pairs (-r) of 80. To look for candidate genes in the QTL for neuromast number, reads that mapped to each Ensembl-predicted gene from Chr XXI were counted using HTSeq 0.5.3p3 (http://www-huber.embl.de/users/anders/HTSeq), with settings --stranded=no and --mode=union.

Differential expression at each age between the two populations was calculated using the Bioconductor package edgeR [89], using the two pools from each population at each age

as sample replicates and following the classic edgeR analysis outlined in the user's guide. A transcript was considered expressed if it had more than 2 reads per kilobase of sequence per million reads mapped (RPKM), and differentially expressed if it had an adjusted $p \geq 0.01$.

For each differentially expressed gene between 3.0 Mb and 7.9 Mb on Chr XXI, a list of single nucleotide polymorphisms (SNPs) between reads from each RNA-seq pool and the reference sequence (Bear Paw Lake, Alaska) was generated using Samtools mpileup [154] with options -IDf and -r. These SNP lists were compared to identify SNPs fixed between PB and JP populations, then the location of those SNPs was manually checked in the RNA-seq pools for the F1 individuals. Allele frequencies were averaged across all SNPs for each gene.

5. Individual gene expression analysis

Purified RNA from each of the individuals collected above was treated with DNase I (Invitrogen, Carlsbad, CA) to remove contamination from genomic DNA, then reverse transcribed into cDNA using the SuperScript III kit (Invitrogen, Carlsbad, CA).

Relative expression of candidate genes in JP and PB fish was determined by performing quantitative PCR (qPCR) on these cDNA samples (see **Table 6-2** for primer sequences,

designed across intron/exon boundaries using Primer Express, Applied Biosystems, Carlsbad, CA), with 3 technical replicates of all samples and 12 biological replicates per age from each population for each tissue type) for each gene. qPCR reactions were carried out and analyzed as described previously [155] using *HPRT* as the reference gene, and calculating primer efficiencies based on a standard curve made from serial dilutions of a pool of JP and PB cDNAs.

Relative expression of PB and JP alleles of each gene in an F1 background was determined using pyrosequencing [91]. Primers were designed around SNPs, identified either by sequencing PCR-amplified copies of candidate genes or by comparison of RNA-seq results from each population, using the PyroMark program (Qiagen, Venlo, Netherlands). PCR fragments were amplified from the cDNA of F1s at 2wph and 4wph (11-12 individuals from each age), as well as from genomic DNA from each of the parents of the cross and an unrelated F1 (as controls to look for biased amplification between alleles) according to the PyroMark kit instructions, and then were sequenced on a PyroMark96 machine. Amplification and sequencing primers are given in **Table 6-3**.

6. Whole mount *in situ* hybridization

Transcripts were amplified from cDNA and subcloned into expression vectors as listed in **Table 6-4**. DIG-labeled sense and antisense probes were generated using a Maxiscript kit (Ambion, Austin, TX) and DIG-labeling mix (Roche Diagnostics, Mannheim, Germany)

using the listed polymerases, and were hydrolyzed to approximately 600 bp. PB and JP fish were collected at 5 days post fertilization (dpf), hatching/10 dpf, 2 weeks post hatching (~12 mm standard length), and 4 weeks post hatching (~17 mm standard length). All fish were fixed overnight at 4°C in 4% paraformaldehyde in 1xPBS, then rinsed briefly in 1x PBS and stored in methanol at -20°C until use. Whole mount *in situ* hybridization was performed as previously described [155].

7. *Eda* transgenics

To make transgenic fish, a plasmid was constructed in which the expression of the JP allele of the *Eda* cDNA was driven by the human cytomegalovirus (CMV) promoter, with Tol2 sites [156] for increased efficiency of transgenesis (**Table 6-5**). The CMV promoter was used because Colosimo et al. [94] previously demonstrated that expression of the mouse *Eda* gene under the control of the same promoter leads to an increase in number of plates in low-plated fish. Constructs were generated by first amplifying the complete *Eda* coding region from JP trunk cDNA (F primer: ATGACACGCGACGGTTCA; R primer: TCAGTTTTGTCCAGCAGATGGA) and cloning it into the pCR-2.1 vector using a TOPO kit (Invitrogen, Carlsbad, CA). This sequence has two variant nucleotide residues compared with the canonical "complete *Eda* allele" shared by most marine sticklebacks that was previously described [94]. Specifically, there was a T->C at bp 95, leading to an amino acid substitution from V->A at position 32, and a G->A at bp 273, leading to a synonymous change. The A1 splice

form was targeted because the *Eda-A1* and *Eda-A2* splice forms bind different receptors in mammals [143], and Colosimo et al. [94] used mouse *Eda-A1* to demonstrate that *Eda* caused ectopic plate formation. To assemble the CMV:*JP-Eda-A1* construct in the Tol2 backbone, the CMV promoter was amplified from the p5E-CMV plasmid in the zebrafish Tol2Kit [157] using a forward primer that contained a 15 bp match with the Tol2 backbone (F primer: ATCACCGGGGGATCCAGGCCTCTTCGCTATTACG; R primer: TCTATAGTGTCACCTAAATCAAGC), amplified *Eda* from the plasmid containing the JP *Eda-A1* cDNA using primers that contained 15 bp matches with the 3' end of the CMV promoter (F primer: AGGTGACACTATAGACCACCATGACACGCGACGGTTCA) and the 5' end of the polyA tail in the Tol2 backbone (R primer: TGGATCATCATCGATTCAGTTTTGTCCAGCAGATGGA), digested the T2-hsp:EGFP plasmid (gift from Tim Howes and David Kingsley) with BamHI and ClaI to remove hsp:EGFP, and combined all three components with InFusion (Clontech, Mountain View, CA). The final plasmid was sequenced to verify all components had expected sequences. Single-cell stickleback embryos were each injected with approximately 1nl of a solution containing 250ng of the CMV:JP-*Eda* plasmid, 350ng RNA encoding the Tol2 transposase enzyme (transcribed *in vitro* using the mMessage mMachine SP6 kit; Ambion, Austin, TX), and 0.1% phenol red (Sigma-Aldrich, St. Louis, MO). Microinjection was carried out as described by Chan et al [79].

Two populations of low-plated *Eda* transgenics were generated: PB pure crosses as well as PBxJP F3 hybrids. Parents for PB crosses were from wild-caught and/or lab-reared stocks. Parents for the PBxJP low-plated F3 fish were F2 offspring from the *in vitro* cross of a PB female to a JP male. Low-plated PBxJP F2s carrying the PB chromosome in the 7 Mb around the *Eda* locus on Chr IV were identified by genotyping with microsatellite markers in *Eda* (*Stn382* at 12.8 Mb [94]) and in flanking regions (*Stn47* at 16.33 Mb [75] and a newly designed marker at 9.01 Mb (Forward primer: GCCATTAGCCAAGGACTATGC; Reverse primer: CCTCTCTGTCCTTCTGTCATCC)). F2s that were found to have only PB (low-plated) alleles in this region were crossed to generate low-plated F3s.

When injected fish were at least 25 mm in standard length, they and their uninjected siblings were stained with calcein. Any injected fish that had more plates on either side than the highest number of plates on any of its uninjected siblings was identified as a putative transgenic. The number of plates on each side was independently assessed, rather than total number of plates, because there was a difference in plate number on opposing sides of individual transgenic fish, probably owing to the mosaic integration of the transgene.

8. Statistical analysis

All statistics for Chapters 2 and 3 were performed using the VassarStats calculators (http://www.vassarstats.net). Mann-Whitney U tests were used to evaluate the effect of sample group on neuromast number, both between original and new fish from the PBxJP cross, and between original PBxJP fish and HTxPB fish. Two-tailed t-tests were used to evaluate differential expression from qPCR data, and Mann-Whitney U tests were used to evaluate allele-specific expression from pyrosequencing data, with Bonferroni corrections for multiple comparisons. Data are reported as means ± standard error.

All statistics for Chapter 4 were performed in R (http://www.R-project.org). Kruskal-Wallis tests were used to evaluate *Eda* qPCR data as well as the effect of transgene and genetic background on plate count. P values reported in the text have been corrected for multiple comparisons. Data are reported as means ± standard error. Fisher Exact test was used to analyze the association between plates and neuromast patterning during development and as a result of transgenic manipulation. The Test of Equality of Proportions was used to assess differences in the percentage of segments with dorso-ventral neuromasts in control *vs.* transgenic fish and between genetic backgrounds.

Table 6-1. Genotyping primers.

Cross	Primer name	Location (Mb)	Forward primer	Reverse primer
HTxPB	Stn222	0.79	TTCCATTTAGATGAAGGCGG	AAGCAGTGGAGAGTTGACCC
	ChrXXI:4.5-1	4.49	GGAGGTTGCTGTTGTCAGG	CGATGGATGCATCATAGAGG
	ChrXXI:5.7-2	5.70	CCTGCTTATCAGCACGTATCC	CGCTGGTATACTGCATGTGG
	ChrXXI:eya1-1	6.83	TTTCACACCCTCCTCTCAGC	TGTTGGGCTTATTCCTTTGG
	ChrXXI:7.9-1	7.87	TGTCCCGTGTCTGTGTCC	AAACACGAGCGACGAACC
	ChrXXI:8.5-1	8.51	CCGGTTTCCAAGATATTACAGC	ACAATGAAGCGTGAGATTCG
PBxJP	Stn222	0.79	TTCCATTTAGATGAAGGCGG	AAGCAGTGGAGAGTTGACCC
	ChrXXI:4.0-1	4.00	ACCTGGGAGCAATTATGTCC	GCTCTGGTAATTGATGTGTTCC
	ChrXXI:4.5-2	4.50	CTTTGAGGTGATGCTTGTGC	ATCTTGGCCTTCTTTCAACC
	ChrXXI:5.7-1	5.69	ACAGCATCTTCATCCTGTTGC	CTCAGAGGAATCGGTGATGC
	ChrXXI:eya1-2	6.84	CATGCTGGGTAAAGAGAGAGC	AGAGGAGCACACTGGAGACC
	ChrXXI:7.9-1	7.87	TGTCCCGTGTCTGTGTCC	AAACACGAGCGACGAACC
	ChrXXI:8.5-2	8.54	AAGTGCATTCAGGGTTCAGC	TGGATTTGTCACTTGGATGG
	ChrXX1:9.0-2	9.03	TCACGTTCTCCATGAAGTGG	TCAATGGGTAAGAGGGATGG
	ChrXXI:9.5-F1	9.48	GGGAGAACTTTCCGTGTTCG	GCTGCAGTTCTTTGTTCTGC

Sequences of primers used to genotype F2 fish at various microsatellites on Chr XXI.

Table 6-2. qPCR primers.

Gene	Location (Mb)	Ensembl gene ID	Forward primer	Reverse primer
BMP6	Chr XXI: 3.83	ENSGACG00000002307	GTCGGCAGGATTGGATCATC	GAGCACTCTCCGTCACAGTAGTTG
TFAP2A	Chr XXI: 4.26	ENSGACG00000002334	AGCATTCCGACCCAAACG	ACTTGCTTCGTGGCCAACAG
novel gene	Chr XXI: 4.34	ENSGACG00000002373	GGCTTCCTCGGCCTCAGT	TCGACACCGTCCTGGAGTTC
MSRB2	Chr XXI: 5.57	ENSGACG00000002478	GATGTACCACTGTGTTTGCTGTGA	CGGTGCCCGAGTCGTACTT
SHARPIN	Chr XXI: 5.79	ENSGACG00000002544	GCCGCGCTCAAGATTCA	GCCAAGTTGATTTCTGTGTCTTCA
CMBL	Chr XXI: 6.01	ENSGACG00000002636	CATTACCTCGCCCTGCAATATC	ACAAAGAGTGTCGGGACCTTCA
SEMA5A	Chr XXI: 6.07	ENSGACG00000002670	ACGCTGGAGGAAAGTGTCAGA	ACGGATAGGGCATTTTGTGATG
CBLN2	Chr XXI: 6.29	ENSGACG00000002693	CAACAGACAAACCATACAGGTGAAC	ACCGGCGAATGCTGATATAACT
SOCS6[1]	Chr XXI: 6.40	ENSGACG00000002698	CCTCCGGATCTCTTCATGGA	GGCAGCGGAACCAAGGA
TRPA1	Chr XXI: 6.76	ENSGACG00000002794	CTTCGCAGGCGCAAAGA	CATACTTCTCTCCGGCCTTCA
Eya1	Chr XXI: 6.83	ENSGACG00000002803	TCATCGTTTTCCATTCCTTGCT	CGGAGGATCCCGTCCATAT
CPA6[1]	Chr XXI: 7.18	ENSGACG00000002857	CTGGACCACGGATCGGTTAT	CCTCTGCAGTGGAACCTGTGA
Eda	Chr IV: 12.80	ENSGACG00000018311	GGAGAGGGTCATGAGGAGAAGTT	GTTATCCTGTGTGGCATGCAA
HPRT	Chr IV: 15.95	ENSGACG00000018634	TCTCCTCCGTTAGAAGACTGCAT	TTCAGGTCATACCCTTGCTCATC

Sequences of the primers used to quantify mRNA levels for each gene; *HPRT* was used as the reference gene. [1]Primers for *SOCS6* and *CPA6* match the PB sequence but contain a SNP to the JP sequence.

Table 6-3. Pyrosequencing primers.

Gene	Location (Mb)	Ensembl Gene ID	Forward primer	Reverse primer	Biotin mod?	Sequencing primer
novel gene	4.34	ENSGACG00000002373	AAAGCCCGAGGCCCTCAC	GGTGGGACTAAGCGTCCAATGT	R	TCAAAGGACCGAATGTA
novel gene	5.18	ENSGACG00000002443	CACTGGTAAAGCAGGAGGAGTCGT	TCATCGCAGAGGCTGTGCT	R	AGCAGGAGGAGTCGT
MSRB2	5.57	ENSGACG00000002478	GAAAGCCACGCCTCCATCAT	GGTCCGGTCCGTCATCAAAC	R	CGTCGCCCTGACAACA
CMBL	6.01	ENSGACG00000002636	AGCTGGATGCAGTGCTGAGG	CCGCTCCGATGTGTTTGG	R	GATGCAGTGCTGAGGT
SOCS6	6.40	ENSGACG00000002698	GGGGGCTGCTACACCAAA	CATCAGGCTCTCGCTCTTG	F	AGCGGCTCTTATTCTG
Eya1	6.83	ENSGACG00000002803	AAGATTCAGATTCGGATCGATTGC	TCTCTTCCATCCTCAGGCCTAAT	R	CAACAACCCTTCCCC
CPA6	7.18	ENSGACG00000002857	AGCCCAACAGCGTAACTTTAAT	ACACCCGATAATCGAGATGCT	R	AATCTGTCAAAATGCAAC

Primers for testing the relative expression of JP and PB alleles from genes on Chr XXI within PBxJP F1 RNA: Forward and Reverse primer sequences, which of those two was modified with Biotin, and the primer used to sequence the Biotin-labeled PCR product.

Table 6-4. *In situ* hybridization primers and conditions.

Gene	Location (Mb)	Ensembl Gene ID	Source	Forward primer	Reverse primer
TROY	Chr I: 4.17	ENSGACG00000006869	Open Biosystems	n/a	n/a
Eya1	Chr XXI: 6.83	ENSGACG00000002803	JP cDNA	ATGGAAATGCAGGATCTAGCC	CTACAAGTACTCCAGGTCCAGC
MSRB2	Chr XXI: 5.57	ENSGACG00000002478	JP cDNA	GGATCCCGGTATTCATTCGT	CAGATTTTCATTTCTAAGCCCTTG
CMBL	Chr XXI: 6.01	ENSGACG00000002636	JP cDNA	CCCGACTTCTACGTTGGAAA	TTTGCAAACAGGAGACAGAGTT
novel gene	Chr XXI: 4.34	ENSGACG00000002373	JP cDNA	GATCTGCACCTCTGCAATCA	CCGGGAGAAAAGACAAACAA

Gene	Vector	Insert length	Hydrol. Time	Antisense RE	Antisense polymerase	Sense RE	Sense polymerase
TROY	pExpress1	~2250	11.1	SmaI	T7	NotI	SP6
Eya1	pCRII-TOPO	1721	9.9	HindIII	T7	EcoRV	SP6
MSRB2	pCR2.1-TOPO	891	5.1	HindIII	T7	HindIII	T7
CMBL	pCRII-TOPO	1068	6.9	HindIII	T7	EcoRV	SP6
novel gene	pCRII-TOPO	1150	7.2	EcoRV	Sp6	BamHI	T7

For each *in situ* hybridization probe used: the source of the plasmid (for *TROY*) or the cDNA from which the gene was amplified and the primers used to amplify it, the plasmid into which it was cloned, and the length of cloned insert. *MSRB2* was cloned twice into pCR2.1-TOPO, once in either direction, to generate separate sense and antisense-generating plasmids. The other genes are all in plasmids from which they can be amplified in either direction (to generate both sense and antisense probes) after linearizing with the restriction enzymes listed and amplifying with the polymerase listed.

Table 6-5. Efficiency of transgenesis.

	PB	PBxJP F3s
Number of clutches screened	11	12
Total fish screened	135	40
Total transgenics identified	27	13

Data on the transgenic fish generated for this study and the efficiency with which they were generated.

References

1. Platt, C., Popper, A., and Fay, R. R. (1989). The ear as part of the octavolateralis system. In The mechanosensory lateral line: neurobiology and evolution, S. Coombs, P. Görner, and H. Münz, eds. (New York: Springer-Verlag), pp. 633–651.

2. Richardson, M. K. (1999). Vertebrate evolution: the developmental origins of adult variation. **Bioessays** *21*, 604–613.

3. Stern, D. L. (2000). Evolutionary developmental biology and the problem of variation. **Evolution** *54*, 1079–1091.

4. Raff, R. A. (1996). The shape of life: genes, development and the evolution of animal form (Chicago: University of Chicago Press).

5. Dijkgraaf, S. S. (1963). The functioning and significance of the lateral-line organs. **Biological Reviews of the Cambridge Philosophical Society** *38*, 51–105.

6. Dijkgraaf, S. S. (1989). A short personal review of the history of lateral line research. In The mechanosensory lateral line: neurobiology and evolution, S. Coombs, P. Görner, and H. Münz, eds. (New York: Springer-Verlag), pp. 7–14.

7. Bleckmann, H. (1986). Role of the lateral line in fish behaviour. In The behaviour of teleost fishes, T. J. Pitcher, ed. (Baltimore: The Johns Hopkins University Press), pp. 177–202.

8. Weissert, R., and Campenhausen, C. (1981). Discrimination between stationary objects by the blind cave fish *Anoptichthys jordani* (Characidae). **Journal of Comparative Physiology A-Neuroethology Sensory Neural and Behavioral Physiology** *143*, 375–381.

9. Hassan, E. S. (1989). Hydrodynamic imaging of the surroundings by the lateral line of the blind cave fish *Anoptichthys jordani*. In The mechanosensory lateral line: neurobiology and evolution, S. Coombs, P. Görner, and H. Münz, eds. (New York: Springer-Verlag), pp. 217–227.

10. Montgomery, J. C., Baker, C. F., and Carton, A. G. (1997). The lateral line can mediate rheotaxis in fish. **Nature** *389*, 960–963.

11. Baker, C. F., and Montgomery, J. C. (1999). Lateral line mediated rheotaxis in the Antarctic fish *Pagothenia borchgrevinki*. **Polar Biology** *21*, 305–309.

12. Kanter, M. J., and Coombs, S. (2003). Rheotaxis and prey detection in uniform currents by Lake Michigan mottled sculpin (*Cottus bairdi*). **Journal of Experimental Biology** *206*, 59–70.

13. Suli, A., Watson, G. M., Rubel, E. W., and Raible, D. W. (2012). Rheotaxis in larval zebrafish is mediated by lateral line mechanosensory hair cells. **PLoS ONE** *7*, e29727.

14. Hoekstra, D., and Janssen, J. (1985). Non-visual feeding behavior of the mottled sculpin, *Cottus bairdi*, in Lake Michigan. **Environmental Biology of Fishes** *12*, 111–117.

15. Montgomery, J. C. (1989). Lateral line detection of planktonic prey. In The mechanosensory lateral line: neurobiology and evolution, S. Coombs, P. Görner, and H. Münz, eds. (New York: Springer-Verlag), pp. 561–574.

16. Montgomery, J. C., and Milton, R. C. (1993). Use of the lateral line for feeding in the torrentfish (*Cheimarrichthys fosteri*). **New Zealand Journal of Zoology** *20*, 121–125.

17. Janssen, J., and Corcoran, J. (1993). Lateral line stimuli can override vision to determine sunfish strike trajectory. **Journal of Experimental Biology** *176*, 299–305.

18. Pohlmann, K., Atema, J., and Breithaupt, T. (2004). The importance of the lateral line in nocturnal predation of piscivorous catfish. **Journal of Experimental Biology** *207*, 2971–2978.

19. Blaxter, J. H. S., and Fuiman, L. A. (1990). The role of the sensory systems of herring larvae in evading predatory fishes. **Journal of Marine Biology** *70*, 413–427.

20. Satou, M., Takeuchi, H. A., Nishii, J., Tanabe, M., Kitamura, S., Okumoto, N., and Iwata, M. (1994). Behavioral and electrophysiological evidences that the lateral line is involved in the inter-sexual vibrational communication of the hime salmon (landlocked red salmon, *Oncorhynchus nerka*). **Journal of Comparative Physiology A** *174*, 539–549.

21. Park, D., Lee, J.-H., Ra, N.-Y., and Eom, J. (2008). Male salamanders *Hynobius leechii* respond to water vibrations via the mechanosensory lateral line system. **Journal of Herpetology** *42*, 615–625.

22. Pitcher, T. J., Partridge, B. L., and Wardle, C. S. (1976). A blind fish can school. **Science** *194*, 963–965.

23. Partridge, B. L., and Pitcher, T. J. (1980). The sensory basis of fish schools: relative roles of lateral line and vision. **Journal of Comparative Physiology A** *135*, 315–325.

24. Faucher, K., Parmentier, E., Becco, C., Vandewalle, N., and Vandewalle, P. (2010). Fish lateral system is required for accurate control of shoaling behaviour. **Animal Behaviour** *79*, 679–687.

25. Brignull, H. R., Raible, D. W., and Stone, J. S. (2009). Feathers and fins: non-mammalian models for hair cell regeneration. **Brain Research** *1277*, 12–23.

26. Kroese, A. B. A., and Van Netten, S. M. (1989). Sensory transduction in lateral line hair cells. In The mechanosensory lateral line: neurobiology and evolution, S. Coombs, P. Görner, and H. Münz, eds. (New York: Springer-Verlag), pp. 265–284.

27. Münz, H. (1989). Functional organization of the lateral line periphery. In The mechanosensory lateral line: neurobiology and evolution, S. Coombs, P. Görner, and H. Münz, eds. (New York: Springer-Verlag), pp. 285–297.

28. Metcalfe, W. K. (1989). Organization and development of the zebrafish posterior lateral line. In The mechanosensory lateral line: neurobiology and evolution, S. Coombs, P. Görner, and H. Münz, eds. (New York: Springer-Verlag), pp. 147–159.

29. Ghysen, A., and Dambly-Chaudière, C. (2004). Development of the zebrafish lateral line. **Current Opinion in Neurobiology** *14*, 67–73.

30. Ghysen, A., and Dambly-Chaudiere, C. (2007). The lateral line microcosmos. **Genes & Development** *21*, 2118–2130.

31. Ma, E. Y., and Raible, D. W. (2009). Signaling pathways regulating zebrafish lateral line development. **Current Biology** *19*, R381–R386.

32. Stone, L. S. (1922). Experiments on the development of the lateral line sense organs in *Amblystoma punctatum*. **Journal of Experimental Zoology** *35*, 421–496.

33. Northcutt, R. G. R., Brändle, K. K., and Fritzsch, B. B. (1995). Electroreceptors and mechanosensory lateral line organs arise from single placodes in axolotls. **Developmental Biology** *168*, 16–16.

34. Schlosser, G. (2002). Development and evolution of lateral line placodes in amphibians I. Development. **Zoology (Jena)** *105*, 119–146.

35. Metcalfe, W. K., Kimmel, C. B., and Schabtach, E. (1985). Anatomy of the posterior lateral line system in young larvae of the zebrafish. **Journal of Comparative Neurology** *233*, 377–389.

36. Kimmel, C. B., Ballard, W. W., Kimmel, S. R., Ullmann, B., and Schilling, T. F. (1995). Stages of embryonic development of the zebrafish. **Developmental Dynamics** *203*, 253–310.

37. Gilmour, D., Knaut, H., Maischein, H.-M., and Nüsslein-Volhard, C. (2004). Towing of sensory axons by their migrating target cells *in vivo*. **Nature Neuroscience** *7*, 491–492.

38. Metcalfe, W. K. (1985). Sensory neuron growth cones comigrate with posterior lateral line primordial cells in zebrafish. **Journal of Comparative Neurology** *238*, 218–224.

39. Lopez-Schier, H., Starr, C. J., Kappler, J. A., Kollmar, R., and Hudspeth, A. J. (2004). Directional cell migration establishes the axes of planar polarity in the posterior lateral-line organ of the zebrafish. **Developmental Cell** *7*, 401–412.

40. Nuñez, V. A., Sarrazin, A. F., Cubedo, N., Allende, M. L., Dambly-Chaudière, C., and Ghysen, A. (2009). Postembryonic development of the posterior lateral line in the zebrafish. **Evolution and Development** *11*, 391–404.

41. Flock, Å., and Wersåll, J. (1962). A study of the orientation of the sensory hairs of the receptor cells in the lateral line organ of fish, with special reference to the function of the receptors. **Journal of Cell Biology** *15*, 19–27.

42. Lopez-Schier, H., and Hudspeth, A. J. (2006). A two-step mechanism underlies the planar polarization of regenerating sensory hair cells. **Proceedings of the National Academy of Sciences of the United States of America** *103*, 18615–18620.

43. Faucherre, A., Pujol-Martí, J., Kawakami, K., and Lopez-Schier, H. (2009). Afferent neurons of the zebrafish lateral line are strict selectors of hair-cell orientation. **PLoS ONE** *4*, e4477.

44. Nagiel, A., Patel, S. H., Andor-Ardo, D., and Hudspeth, A. J. (2009). Activity-independent specification of synaptic targets in the posterior lateral line of the larval zebrafish. **Proceedings of the National Academy of Sciences of the United States of America** *106*, 21948–21953.

45. Fame, R. M., Brajon, C., and Ghysen, A. (2006). Second-order projection from the posterior lateral line in the early zebrafish brain. **Neural Development** *1*, 4.

46. Sapède, D., Gompel, N., Dambly-Chaudière, C., and Ghysen, A. (2002). Cell migration in the postembryonic development of the fish lateral line. **Development** *129*, 605–615.

47. Ghysen, A., Schuster, K., Coves, D., la Gandara, de, F., Papandroulakis, N., and Ortega, A. (2010). Development of the posterior lateral line system in *Thunnus thynnus*, the atlantic blue-fin tuna, and in its close relative *Sarda sarda*. **International Journal of Developmental Biology** *54*, 1317–1322.

48. Ghysen, A., Dambly-Chaudière, C., Coves, D., la Gandara, de, F., and Ortega, A. (2012). Developmental origin of a major difference in sensory patterning between zebrafish and bluefin tuna. **Evolution and Development** *14*, 204–211.

49. Ledent, V. (2002). Postembryonic development of the posterior lateral line in zebrafish. **Development** *129*, 597–604.

50. Grant, K. A., Raible, D. W., and Piotrowski, T. (2005). Regulation of latent sensory hair cell precursors by glia in the zebrafish lateral line. **Neuron** *45*, 69–80.

51. Lopez-Schier, H., and Hudspeth, A. J. (2005). Supernumerary neuromasts in the posterior lateral line of zebrafish lacking peripheral glia. **Proceedings of the National Academy of Sciences of the United States of America** *102*, 1496–1501.

52. Wada, H., Ghysen, A., Asakawa, K., Abe, G., Ishitani, T., and Kawakami, K. (2013). Wnt/Dkk negative feedback regulates sensory organ size in zebrafish. **Current Biology** *23*, 1559–1565.

53. Pichon, F., and Ghysen, A. (2004). Evolution of posterior lateral line development in fish and amphibians. **Evolution and Development** *6*, 187–193.

54. Coombs, S., Janssen, J., and Webb, J. F. (1988). Diversity of lateral line systems: evolutionary and functional considerations. In Sensory Biology of Aquatic Animals, J. Atema, R. R. Fay, and A. Popper, eds. (Berlin: Springer), pp. 553–593.

55. Webb, J. F. (1989). Gross morphology and evolution of the mechanoreceptive lateral-line system in teleost fishes. **Brain, Behavior and Evolution** *33*, 34–53.

56. Vischer, H. A. (1990). The morphology of the lateral line system in 3 species of Pacific cottoid fishes occupying disparate habitats. **Experientia** *46*, 244–250.

57. Carton, A., and Montgomery, J. (2004). A comparison of lateral line morphology of blue cod and torrentfish: two sandperches of the family Pinguipedidae. **Environmental Biology of Fishes** *70*, 123–131.

58. Wark, A. R., and Peichel, C. L. (2010). Lateral line diversity among ecologically divergent threespine stickleback populations. **Journal of Experimental Biology** *213*, 108–117.

59. Wellenreuther, M., Brock, M., Montgomery, J., and Clements, K. D. (2010). Comparative morphology of the mechanosensory lateral line system in a clade of New Zealand triplefin fishes. **Brain, Behavior and Evolution** *75*, 292–308.

60. Fischer, E. K., Soares, D., Archer, K. R., Ghalambor, C. K., and Hoke, K. L. (2013). Genetically and environmentally mediated divergence in lateral line morphology in the Trinidadian guppy (*Poecilia reticulata*). **Journal of Experimental Biology**, doi:10.1242–jeb.081349.

61. Teyke, T. (1990). Morphological differences in neuromasts of the blind cave fish *Astyanax hubbsi* and the sighted river fish *Astyanax mexicanus*. **Brain, Behavior and Evolution** *35*, 23–30.

62. Trokovic, N., Herczeg, G., McCairns, R. J. S., Ghani, N Izza AB, and Merilä, J. (2011). Intraspecific divergence in the lateral line system in the nine-spined stickleback (*Pungitius pungitius*). **Journal of Evolutionary Biology** *24*, 1546–1558.

63. Webb, J. F. (1989). Developmental constraints and evolution of the lateral line system in teleost fishes. In The mechanosensory lateral line: neurobiology and evolution, S. Coombs, P. Görner, and H. Münz, eds. (New York: Springer-Verlag), pp. 79–97.

64. Gould, S. J. S., and Lewontin, R. C. R. (1979). The spandrels of San Marco and the Panglossian paradigm: a critique of the adaptationist programme. Proceedings of the Royal Society of London Series B-Biological Sciences *205*, 581–598.

65. Northcutt, R. G. (1988). Sensory and other neural traits and the adaptionist program: mackerels of San Marco? In Sensory biology of aquatic animals, J. Atema, R. R. Fay, A. N. Popper, and W. N. Tavolga, eds. (New York: Springer-Verlag), pp. 870–883.

66. Barrett, R. D. H., and Hoekstra, H. E. (2011). Molecular spandrels: tests of adaptation at the genetic level. Nature Reviews Genetics *12*, 767–780.

67. Engeszer, R. E., Patterson, L. B., Rao, A. A., and Parichy, D. M. (2007). Zebrafish in the wild: a review of natural history and new notes from the field. **Zebrafish** *4*, 21–40.

68. Jeffery, W. R., Strickler, A. G., Guiney, S., Heyser, D. G., and Tomarev, S. I. (2000). *Prox 1* in eye degeneration and sensory organ compensation during development and evolution of the cavefish *Astyanax*. **Development Genes and Evolution** *210*, 223–230.

69. Wark, A. R., Mills, M. G., Dang, L. H., Chan, Y. F., Jones, F. C., Brady, S. D., Absher, D. M., Grimwood, J., Schmutz, J., Myers, R. M., et al. (2012). Genetic architecture of variation in the lateral line sensory system of threespine sticklebacks. **G3: Genes| Genomes| Genetics** *2*, 1047–1056.

70. Bell, M. A., and Foster, S. A. (1994). The evolutionary biology of the threespine stickleback (Oxford: Oxford University Press).

71. Schluter, D., Marchinko, K. B., Barrett, R. D. H., and Rogers, S. M. (2010). Natural selection and the genetics of adaptation in threespine stickleback. **Philosophical Transactions of the Royal Society B: Biological Sciences** *365*, 2479–2486.

72. Bell, M. A. (1987). Interacting evolutionary constraints in pelvic reduction of threespine sticklebacks, *Gasterosteus aculeatus* (Pisces, Gasterostedae). **Biological Journal of the Linnean Society** *31*, 347–382.

73. Cresko, W. A., Amores, A., Wilson, C., Murphy, J., Currey, M., Phillips, P., Bell, M. A., Kimmel, C. B., and Postlethwait, J. H. (2004). Parallel genetic basis for repeated evolution of armor loss in Alaskan threespine stickleback populations. **Proceedings of the National Academy of Sciences of the United States of America** *101*, 6050–6055.

74. Barrett, R. D. H. (2010). Adaptive evolution of lateral plates in three-spined stickleback *Gasterosteus aculeatus*: a case study in functional analysis of natural variation. **Journal of Fish Biology** *77*, 311–328.

75. Peichel, C. L., Nereng, K. S., Ohgi, K. A., Cole, B. L., Colosimo, P. F., Buerkle, C. A., Schluter, D., and Kingsley, D. M. (2001). The genetic architecture of divergence between threespine stickleback species. **Nature** *414*, 901–905.

76. Jones, F. C., Chan, Y. F., Schmutz, J., Grimwood, J., Brady, S. D., Southwick, A. M., Absher, D. M., Myers, R. M., Reimchen, T. E., Deagle, B. E., et al. (2012). A genome-wide SNP genotyping array reveals patterns of global and repeated species-pair divergence in sticklebacks. **Current Biology** *22*, 83–90.

77. Jones, F. C., Grabherr, M. G., Chan, Y. F., Russell, P., Mauceli, E., Johnson, J., Swofford, R., Pirun, M., Zody, M. C., White, S., et al. (2012). The genomic basis of adaptive evolution in threespine sticklebacks. **Nature** *484*, 55–61.

78. Miller, C. T., Beleza, S., Pollen, A. A., Schluter, D., Kittles, R. A., Shriver, M. D., and Kingsley, D. M. (2007). *Cis*-regulatory changes in *Kit ligand* expression and parallel evolution of pigmentation in sticklebacks and humans. **Cell** *131*, 11–11.

79. Chan, Y. F., Marks, M. E., Jones, F. C., Villarreal, G., Shapiro, M. D., Brady, S. D., Southwick, A. M., Absher, D. M., Grimwood, J., Schmutz, J., et al. (2010). Adaptive evolution of pelvic reduction in sticklebacks by recurrent deletion of a *Pitx1* enhancer. **Science** *327*, 302–305.

80. Colosimo, P. F., Peichel, C. L., Nereng, K., Blackman, B. K., Shapiro, M. D., Schluter, D., and Kingsley, D. M. (2004). The genetic architecture of parallel armor plate reduction in threespine sticklebacks. **PLoS Biology** *2*, e109.

81. Shapiro, M. D., Marks, M. E., Peichel, C. L., Blackman, B. K., Nereng, K. S., Jónsson, B., Schluter, D., and Kingsley, D. M. (2004). Genetic and developmental basis of evolutionary pelvic reduction in threespine sticklebacks. **Nature** *428*, 717–723.

82. Albert, A. Y. K., Sawaya, S., Vines, T. H., Knecht, A. K., Miller, C. T., Summers, B. R., Balabhadra, S., Kingsley, D. M., and Schluter, D. (2008). The genetics of adaptive shape shift in stickleback: pleiotropy and effect size. **Evolution** *62*, 76–85.

83. Kitano, J., Ross, J. A., Mori, S., Kume, M., Jones, F. C., Chan, Y. F., Absher, D. M., Grimwood, J., Schmutz, J., Myers, R. M., et al. (2009). A role for a neo-sex chromosome in stickleback speciation. **Nature** *461*, 1079–1083.

84. Greenwood, A. K., Jones, F. C., Chan, Y. F., Brady, S. D., Absher, D. M., Grimwood, J., Schmutz, J., Myers, R. M., Kingsley, D. M., and Peichel, C. L. (2011). The genetic basis of divergent pigment patterns in juvenile threespine sticklebacks. **Heredity (Edinb)** *107*, 155–166.

85. Honkanen, T. (1993). Comparative study of the lateral-line system of the three-spined stickleback (*Gasterosteus aculeatus*) and the nine-spined stickleback (*Pungitius pungitius*). **Acta Zoologica** *74*, 331–336.

86. Reimchen, T. E., Bergstrom, C., and Nosil, P. (2013). Natural selection and the adaptive radiation of Haida Gwaii stickleback. **Evolutionary Ecology Research** *15*, 241–269.

87. Bell, M. A., and Aguirre, W. (2013). Contemporary evolution, allelic recycling, and adaptive radiation of the threespine stickleback. **Evolutionary Ecology Research** *15*, 377–411.

88. Shapiro, M. D., Marks, M. E., Peichel, C. L., Blackman, B. K., Nereng, K. S., Jónsson, B., Schluter, D., and Kingsley, D. M. (2004). Genetic and developmental basis of evolutionary pelvic reduction in threespine sticklebacks. **Nature** *428*, 717–723.

89. Robinson, M. D., McCarthy, D. J., and Smyth, G. K. (2009). edgeR: a Bioconductor package for differential expression analysis of digital gene expression data. **Bioinformatics** *26*, 139–140.

90. Trapnell, C., Pachter, L., and Salzberg, S. L. (2009). TopHat: discovering splice junctions with RNA-Seq. **Bioinformatics** *25*, 1105–1111.

91. Nordström, T., Ronaghi, M., Forsberg, L., de Faire, U., Morgenstern, R., and Nyrén, P. (2000). Direct analysis of single-nucleotide polymorphism on double-stranded DNA by pyrosequencing. **Biotechnology & Applied Biochemistry** *31*, 107–112.

92. Kozlowski, D. J., Whitfield, T. T., Hukriede, N. A., Lam, W. K., and Weinberg, E. S. (2005). The zebrafish *dog-eared* mutation disrupts *eya1*, a gene required for cell survival and differentiation in the inner ear and lateral line. **Developmental Biology** *277*, 27–41.

93. Knecht, A. K. A., Hosemann, K. E. K., and Kingsley, D. M. D. (2007). Constraints on utilization of the EDA-signaling pathway in threespine stickleback evolution. **Evolution and Development** *9*, 141–154.

94. Colosimo, P. F., Hosemann, K. E., Balabhadra, S., Villarreal, G., Dickson, M. C., Grimwood, J., Schmutz, J., Myers, R. M., Schluter, D., and Kingsley, D. M. (2005). Widespread parallel evolution in sticklebacks by repeated fixation of *Ectodysplasin* alleles. **Science** *307*, 1928–1933.

95. Sahly, I., Andermann, P., and Petit, C. (1999). The zebrafish *eya1* gene and its expression pattern during embryogenesis. **Development Genes and Evolution** *209*, 399–410.

96. Thisse, B., and Thisse, C. (2004). Fast release clones: a high throughput expression analysis. zfin.org. Available at: http://zfin.org [Accessed July 17, 2013].

97. Pascual, I., Larrayoz, I. M., Campos, M. M., and Rodriguez, I. R. (2010). Methionine sulfoxide reductase B2 is highly expressed in the retina and protects retinal pigmented epithelium cells from oxidative damage. **Experimental Eye Research** *90*, 420–428.

98. Ishizuka, T., Fujimori, I., Kato, M., Noji-Sakikawa, C., Saito, M., Yoshigae, Y., Kubota, K., Kurihara, A., Izumi, T., Ikeda, T., et al. (2010). Human carboxymethylenebutenolidase as a bioactivating hydrolase of olmesartan medoxomil in liver and intestine. **Journal of Biological Chemistry** *285*, 11892–11902.

99. Xia, T., Liang, Y., Ma, J., Li, M., Gong, M., and Yu, X. (2010). Loss-of-function of SHARPIN causes an osteopenic phenotype in mice. **Endocrinology** *39*, 104–112.

100. Landgraf, K., Bollig, F., Trowe, M. O., Besenbeck, B., Ebert, C., Kruspe, D., Kispert, A., Hanel, F., and Englert, C. (2010). Sipl1 and Rbck1 are novel Eya1-binding proteins with a role in craniofacial development. **Molecular and Cellular Biology** *30*, 5764–5775.

101. Trapnell, C., Roberts, A., Goff, L., Pertea, G., Kim, D., Kelley, D. R., Pimentel, H., Salzberg, S. L., Rinn, J. L., and Pachter, L. (2012). Differential gene and transcript expression analysis of RNA-seq experiments with TopHat and Cufflinks. **Nature Protocols** *7*, 562–578.

102. Fisher, R. A. (1930). The genetical theory of natural selection (Oxford: Oxford University Press).

103. Orr, H. A. (2000). Adaptation and the cost of complexity. **Evolution** *54*, 13–20.

104. Schluter, D. (2000). The ecology of adaptive radiation (Oxford: Oxford University Press).

105. Lande, R. (1979). Quantitative genetic analysis of multivariate evolution, applied to brain: body size allometry. **Evolution** *33*, 402–416.

106. Kirkpatrick, M., and Barton, N. (2006). Chromosome inversions, local adaptation and speciation. **Genetics** *173*, 419–434.

107. Hoffmann, A. A., and Rieseberg, L. H. (2008). Revisiting the impact of inversions in evolution: from population genetic markers to drivers of adaptive shifts and speciation? **Annual Review of Ecology Evolution and Systematics** *39*, 21–42.

108. Hawthorne, D. J., and Via, S. (2001). Genetic linkage of ecological specialization and reproductive isolation in pea aphids. **Nature** *412*, 904–907.

109. Albertson, R. C., Streelman, J. T., and Kocher, T. D. (2003). Directional selection has shaped the oral jaws of Lake Malawi cichlid fishes. **Proceedings of the National Academy of Sciences of the United States of America** *100*, 5252–5257.

110. Bratteler, M. M., Lexer, C. C., and Widmer, A. A. (2006). Genetic architecture of traits associated with serpentine adaptation of *Silene vulgaris*. **Journal of Evolutionary Biology** *19*, 1149–1156.

111. Hall, M. C., Basten, C. J., and Willis, J. H. (2006). Pleiotropic quantitative trait loci contribute to population divergence in traits associated with life-history variation in *Mimulus guttatus*. **Genetics** *172*, 1829–1844.

112. Protas, M., Tabansky, I., Conrad, M., Gross, J. B., Vidal, O., Tabin, C. J., and Borowsky, R. (2008). Multi-trait evolution in a cave fish, *Astyanax mexicanus*. **Evolution and Development** *10*, 196–209.

113. Lowry, D. B., and Willis, J. H. (2010). A widespread chromosomal inversion polymorphism contributes to a major life-history transition, local adaptation, and reproductive isolation. **PLoS Biology** *8*, e1000500.

114. Joron, M., Frezal, L., Jones, R. T., Chamberlain, N. L., Lee, S. F., Haag, C. R., Whibley, A., Becuwe, M., Baxter, S. W., Ferguson, L., Wilkinson, P. A., Salazar, C., Davidson, C., Clark, R. Quail, M. A., Beasley, H., Glithero, R., Lloyd, C., Sims, S., Jones, M. C., Rogers, J., Jiggins, C. D., ffrench-Constant, R. H. (2011). Chromosomal rearrangements maintain a polymorphic supergene controlling butterfly mimicry. **Nature** *477*, 203–206.

115. Parnell, N. F., Hulsey, C. D., and Streelman, J. T. (2012). The genetic basis of a complex functional system. **Evolution** *66*, 3352–3366.

116. Hermann, K., Klahre, U., Moser, M., Sheehan, H., Mandel, T., and Kuhlemeier, C. (2013). Tight genetic linkage of prezygotic barrier loci creates a multifunctional speciation island in *Petunia*. **Current Biology** *23*, 873–877.

117. Phillips, P. C. (2005). Testing hypotheses regarding the genetics of adaptation. **Genetica** *123*, 15–24.

118. Flint, J., and Mackay, T. F. C. (2009). Genetic architecture of quantitative traits in mice, flies, and humans. **Genome Research** *19*, 723–733.

119. Wittkopp, P. J., and Beldade, P. (2009). Development and evolution of insect pigmentation: genetic mechanisms and the potential consequences of pleiotropy. **Seminars in Cell and Developmental Biology** *20*, 65–71.

120. Kingsley, D. M., and Peichel, C. L. (2007). The molecular genetics of evolutionary change in sticklebacks. In Biology of the three-spined stickleback, S. Östlund-Nilsson, I. Mayer, and F. Huntingford, eds. (Boca Raton: CRC Press), pp. 41–81.

121. Bell, M. A. (1981). Lateral plate polymorphism and ontogeny of the complete plate morph of threespine sticklebacks (*Gasterosteus aculeatus*). **Evolution** *35*, 67–74.

122. Graham-Smith, W. (1978). On the lateral lines and dermal bones in the parietal region of some crossopterygian and dipnoan fishes. **Philosophical Transactions of the Royal Society of London. Series B, Biological Sciences** *282*, 41–105.

123. de Beer, G. R. (1937). The Development of the Vertebrate Skull (Oxford: Clarendon Press).

124. Wada, H., Ghysen, A., Satou, C., Higashijima, S.-I., Kawakami, K., Hamaguchi, S., and Sakaizumi, M. (2010). Dermal morphogenesis controls lateral line patterning during postembryonic development of teleost fish. **Developmental Biology** *340*, 583–594.

125. Hendry, A. P., Peichel, C. L., Matthews, B., Boughman, J. W., and Nosil, P. (2013). Stickleback research: the now and the next. **Evolutionary Ecology Research** *15*, 111–141.

126. Malek, T. B., Boughman, J. W., Dworkin, I., and Peichel, C. L. (2012). Admixture mapping of male nuptial colour and body shape in a recently formed hybrid population of threespine stickleback. **Molecular Ecology** *21*, 5265–5279.

127. Rogers, S. M. S., Tamkee, P. P., Summers, B. B., Balabahadra, S. S., Marks, M. M., Kingsley, D. M. D., and Schluter, D. D. (2012). Genetic signature of adaptive peak shift in threespine stickleback. **Evolution** *66*, 2439–2450.

128. Barrett, R. D. H., Rogers, S. M., and Schluter, D. (2008). Natural selection on a major armor gene in threespine stickleback. **Science** *322*, 255–257.

129. Barrett, R. D. H., Rogers, S. M., and Schluter, D. (2009). Environment specific pleiotropy facilitates divergence at the *Ectodysplasin* locus in threespine stickleback. **Evolution** *63*, 2831–2837.

130. Barrett, R. D. H., Vines, T. H., Bystriansky, J. S., and Schulte, P. M. (2009). Should I stay or should I go? The *Ectodysplasin* locus is associated with behavioural differences in threespine stickleback. **Biology Letters** *5*, 788–791.

131. Greenwood, A. K., Wark, A. R., Yoshida, K., and Peichel, C. L. (2013). Genetic and neural modularity underlie the evolution of schooling behavior in threespine sticklebacks. **Current Biology**, in press.

132. Marchinko, K. B. (2009). Predation's role in repeated phenotypic and genetic divergence of armor in threespine stickleback. **Evolution** *63*, 127–138.

133. Le Rouzic, A., Østbye, K., Klepaker, T. O., Hansen, T. F., Bernatchez, L., Schluter, D., and Vøllestad, L. A. (2011). Strong and consistent natural selection associated with armour reduction in sticklebacks. **Molecular Ecology** *20*, 2483–2493.

134. Philip, S., Machado, J. P., Maldonado, E., Vasconcelos, V., O'Brien, S. J., Johnson, W. E., and Antunes, A. (2012). Fish lateral line innovation: insights into the evolutionary genomic dynamics of a unique mechanosensory organ. **Molecular Biology and Evolution** *29*, 3887–3898.

135. Villablanca, E. J., Renucci, A., Sapède, D., Lec, V., Soubiran, F., Sandoval, P. C., Dambly-Chaudière, C., Ghysen, A., and Allende, M. L. (2006). Control of cell migration in the zebrafish lateral line: Implication of the gene "tumour-associated calcium signal transducer," *tacstd*. **Developmental Dynamics** *235*, 1578–1588.

136. Smith, S. C., Lannoo, M. J., and Armstrong, J. B. (1990). Development of the mechanoreceptive lateral-line system in the axolotl: placode specification, guidance of migration, and the origin of neuromast polarity. **Anatomy and Embryology (Berlin)** *182*, 171–180.

137. Blaxter, J. H. S., Gray, J. A. B., and Best, A. C. G. (1983). Structure and development of the free neuromasts and lateral line system of the herring. **Journal of the Marine Biology Association of the U.K.** *63*, 247–260.

138. Mohr, C., and Görner, P. (1996). Innervation patterns of the lateral line stitches of the clawed frog, *Xenopus laevis*, and their reorganization during metamorphosis. **Brain, Behavior and Evolution** *48*, 55–69.

139. Leinonen, T., McCairns, R. J. S., Herczeg, G., and Merilä, J. (2012). Multiple evolutionary pathways to decreased lateral plate coverage in freshwater threespine sticklebacks. **Evolution** *66*, 3866–3875.

140. Pehrson, T. (1944). Some observations on the development and morphology of the dermal bones in the skull of acipenser and polyodon. **Acta Zoologica** *Bd. 25*, 27–48.

141. Graham-Smith, W. (1978). On some variations in the latero-sensory lines of the placoderm fish *Bothriolepis*. **Philosophical Transactions of the Royal Society B: Biological Sciences** *282*, 1–39.

142. Hernández, P. P., Moreno, V., Olivari, F. A., and Allende, M. L. (2006). Sub-lethal concentrations of waterborne copper are toxic to lateral line neuromasts in zebrafish (*Danio rerio*). **Hearing Research** *213*, 1–10.

143. Yan, M., Wang, L.-C., Hymowitz, S. G., Schilbach, S., Lee, J., Goddard, A., de Vos, A. M., Gao, W.-Q., and Dixit, V. M. (2000). Two-amino acid molecular switch in an epithelial morphogen that regulates binding to two distinct receptors. **Science** *290*, 523–527.

144. Kondo, Kuwahara, Kondo, Naruse, Mitani, Wakamatsu, Ozato, Asakawa, Shimizu, Shima (2001). The medaka *rs-3* locus required for scale development encodes ectodysplasin-A receptor. **Current Biology** *11*, 5–5.

145. Atukorala, A. D. S., Inohaya, K., Baba, O., Tabata, M. J., Ratnayake, R. A. R. K., Abduweli, D., Kasugai, S., Mitani, H., and Takano, Y. (2010). Scale and tooth phenotypes in medaka with a mutated ectodysplasin-A receptor: implications for the evolutionary origin of oral and pharyngeal teeth. **Archives of Histology and Cytology** *73*, 139–148.

146. Cui, C.-Y., and Schlessinger, D. (2006). EDA signaling and skin appendage development. **Cell Cycle** *5*, 2477–2483.

147. Moore, F. E., Reyon, D., Sander, J. D., Martinez, S. A., Blackburn, J. S., Khayter, C., Ramirez, C. L., Joung, J. K., and Langenau, D. M. (2012). Improved somatic mutagenesis in zebrafish using transcription activator-like effector nucleases (TALENs). **PLoS ONE** *7*, e37877.

148. Kitano, J., Bolnick, D. I., Beauchamp, D. A., Mazur, M. M., Mori, S., Nakano, T., and Peichel, C. L. (2008). Reverse Evolution of Armor Plates in the Threespine Stickleback. **Current Biology** *18*, 769–774.

149. Tinbergen, N. (1951). The study of instinct (Oxford: Oxford University Press).

150. Huntingford, F. A., and Ruiz-Gomez, M. L. (2009). Three-spined sticklebacks *Gasterosteus aculeatus* as a model for exploring behavioural biology. **Journal of Fish Biology** *75*, 1943–1976.

151. Wark, A. R., Greenwood, A. K., Taylor, E. M., Yoshida, K., and Peichel, C. L. (2011). Heritable differences in schooling behavior among threespine stickleback populations revealed by a novel assay. **PLoS ONE** *6*, e18316.

152. Koressaar, T., and Remm, M. (2007). Enhancements and modifications of primer design program Primer3. **Bioinformatics** *23*, 1289–1291.

153. Untergasser, A., Cutcutache, I., Koressaar, T., Ye, J., Faircloth, B. C., Remm, M., and Rozen, S. G. (2012). Primer3--new capabilities and interfaces. **Nucleic Acids Research** *40*, e115–e115.

154. Li, H., Handsaker, B., Wysoker, A., Fennell, T., Ruan, J., Homer, N., Marth, G., Abecasis, G., Durbin, R., and 1000 Genome Project Data Processing Subgroup (2009). The Sequence Alignment/Map format and SAMtools. **Bioinformatics** *25*, 2078–2079.

155. Greenwood, A. K., Cech, J. N., and Peichel, C. L. (2012). Molecular and developmental contributions to divergent pigment patterns in marine and freshwater sticklebacks. **Evolution and Development** *14*, 351–362.

156. Kawakami, K., Shima, A., and Kawakami, N. (2000). Identification of a functional transposase of the *Tol2* element, an *Ac*-like element from the Japanese medaka fish, and its transposition in the zebrafish germ lineage. **Proceedings of the National Academy of Sciences of the United States of America** *97*, 11403–11408.

157. Kwan, K. M., Fujimoto, E., Grabher, C., Mangum, B. D., Hardy, M. E., Campbell, D. S., Parant, J. M., Yost, H. J., Kanki, J. P., and Chien, C.-B. (2007). The Tol2kit: A multisite gateway-based construction kit for *Tol2* transposon transgenesis constructs. **Developmental Dynamics** *236*, 3088–3099.